MULTIBAND TRIANGULAR PATCH ANTENNA

A Dissertation submitted towards the partial fulfilment of the requirement for the award of the degree of

Master of Technology

in

Microwave and Optical Communication Engineering

Submitted by

Prateek Srivastava

2K11/MOC/09

Under the supervision of

Dr. Priyanka Jain

(Assistant Professor)

Department of Electronics & Communication Engineering

DEPARTMENT OF
ELECTRONICS & COMMUNICATION ENGINEERING
AND
APPLIED PHYSICS

DELHI TECHNOLOGICAL UNIVERSITY
(FORMERLY DELHI COLLEGE OF ENGINEERING)
NEW DELHI-110042

JUNE 2013

CERTIFICATE

This is to certify that the thesis report entitled, "**Multiband Triangular Patch Antenna**" being submitted by **Prateek Srivastava** to the *Department of Electronics and Communication Engineering and Applied Physics*, ***Delhi Technological University*** in partial fulfilment of the requirement for award of Master of Technology degree in ***Microwave and Optical Communication*** is a record of bona fide work carried out by him under the supervision and guidance of **Dr. Priyanka Jain.** The matter embodied in this report has not been submitted to any other University/ Institute the award of any other degree.

Dr. Priyanka Jain
Supervisor
Assistant Professor(ECE)
Delhi Technological
University, New Delhi

Prof. Rajiv Kapoor
Head of Department
Deptt. of ECE
Delhi Technological
University, New Delhi

Prof. S.C.Sharma
Head of Department
Deptt.of Applied Physics
Delhi Technological
University, New Delhi

DECLARATION

I hereby declare that all the information in this document has been obtained and presented in accordance with academic rules and ethical conduct. This report is my own, unaided work. I have fully cited and referenced all material and results that are not original to this work. It is being submitted for the degree of Master of Technology in Engineering at the Delhi Technological University. It has not been submitted before for any degree or examination in any other university.

Name : Prateek Srivastava

Signature :

ABSTRACT

In telecommunication, there are several types of microstrip antennas (also known as printed antennas) the most common of which is the microstrip patch antenna or patch antenna. A patch antenna is a narrowband, wide-beam antenna.

Microstrip antennas are relatively inexpensive to manufacture and design because of the simple 2-dimensional physical geometry. They are usually employed at UHF and higher frequencies because the size of the antenna is directly tied to the wavelength at the resonant frequency. A single patch antenna provides a maximum directive gain of around 6-9 dB. It is relatively easy to print an array of patches on a single (large) substrate using lithographic techniques. Patch arrays can provide much higher gains than a single patch at little additional cost; matching and phase adjustment can be performed with printed microstrip feed structures, again in the same operations that form the radiating patches. The ability to create high gain arrays in a low-profile antenna is one reason that patch arrays are common on airplanes and in other military applications

The most commonly employed microstrip antenna is a rectangular patch. The rectangular patch antenna is approximately a one-half wavelength long section of rectangular microstrip transmission line. When air is the antenna substrate, the length of the rectangular microstrip antenna is approximately one-half of a free-space wavelength. As the antenna is loaded with a dielectric as its substrate, the length of the antenna decreases as the relative dielectric constant of the substrate increases. Here a rectangular patch antenna resonating at 2.4 GHz is designed and their reflection coefficient, radiation pattern & polar plot is drawn & analysed. Now the Triangular patch antenna working on same resonant frequency is designed which is having less size compared to the rectangular patch antenna.

The triangular microstrip antenna is one of the shapes of microstrip antennas which have radiation properties similar to that of the rectangular antenna but with the advantage of being physically smaller. The simplest of triangular shapes is equilateral antenna which has more directivity with compact size.

In this project rectangular patch has been designed to operate at resonance frequency of 2.4 GHz for Wi-Fi application. Then a triangular patch antenna of same resonating frequency is designed. It has been seen from the result that the size required for the triangular antenna to resonate at the same frequency is less as compared to rectangular patch antenna.

Then triangular slots have been made in the same triangular patch antenna so that it is converted into the fractal antenna and the design is simulated. The result obtained for two fractal geometry shows that the return loss of the antenna at 2.4 GHz is less as compared to the same dimensions of triangular patch antenna. Fractal antenna is having many advantages over the simple patch antenna like miniaturization, better input impedance matching & wideband / multiband behaviour.

A new triangular multiband patch antenna has been designed to operate at resonant frequencies 1.1 GHz, 2 GHz & 3 GHz.. again the triangular slots are cut in this design to make it fractal antenna so we get the lower return loss at resonant frequencies.

ACKNOWLEDGEMENT

I would like to express my sincere gratitude to my project supervisor, **Dr. Priyanka Jain**, for her supervision, invaluable guidance, motivation and support throughout the extent of the project. I have benefitted immensely from her wealth of knowledge.

I am deeply grateful to **Prof. Rajiv Kapoor**, Head of Department of Electronics and Communication Engineering, Delhi Technological University for his support and encouragement in carrying out this project.

I would also like to thank **Dr.R.K.Sinha**, Professor and **Dr. Ajeet Kumar,** Assistant Professor, Department of Applied Physics, Delhi Technological University, for their precious suggestions, support and technical help during the course of this project.

I wish to express my heart full thanks to **Prof. S.C. Sharma**, Head of Department of Applied Physics, Delhi Technological University for his support that helped me a lot in successful completion of this project.

I am also grateful to **Prof. P. B. Sharma,** Vice-Chancellor, Delhi Technological University for providing the research environment in the institute.

I would like to express my heartiest thank to my colleagues and friends for constant support and motivation. Last but not least I thank my parents, for everything I am and will be in future. It's your unspoken prayers and affection that keep me moving forward.

Prateek Srivastava
M.tech(MOCE)
2K11/MOC/09

TABLE OF CONTENTS

LIST OF FIGURES

LIST OF TABLES

LIST OF ABBREVIATIONS

HFSS	:	High Frequency Structure Simulator
E_θ	:	The θ component of the electric field
E_Φ	:	The Φ component of the electric field
HPBW	:	Half Power Beamwidth
FNBW	:	Full Null Beamwidth
BE	:	Beam Efficiency
$D(\theta,\Phi)$	:	Directivity
$U(\theta,\Phi)$	:	Radiation Intensity
Ω	:	Solid Angle
Q	:	Quality Factor
P_r	:	Radiated Power
η_t	:	Total Antenna Efficiency
η_r	:	Radiation Efficiency
□	:	Voltage Reflection Coefficient
h	:	Height of Dielectric Substrate
W	:	Width of Patch
L	:	Length of Patch
t	:	Open circuit Stub
λ	:	Wavelength
λ_o	:	Free space Wavelength
ε_{eff}	:	Effective Dielectric Constant
ε_r	:	Dielectric Constant of Substrate
L_{eff}	:	Effective Length of The Patch
f_0	:	Resonance Frequency
tanδ	:	Loss Tangent Of The Dielectric.
δ_{eff}	:	Effective Loss Tangent
C^*_{dyn}	:	Complex Dynamic Capacitance of Equivalent Rectangular Patch
f_{mn}	:	Resonant Frequency For Higher Order Modes
Z_{in}	:	Input Impedance
ε	:	Permittivity of The Substrate

μo	:	Permittivity of Free Space
J	:	Current Density Due to the Feed

Chapter 1

Introduction

1.1 Introduction

The radio antenna is a primary component in all radio systems. It may be defined as the structure associated with the region of transition between a guided wave and a free space wave, or vice versa [1]. In other words, radio antennas couple electromagnetic energy from one medium (space) to another (e.g. wire, coaxial cable, or wave guide). The increasing demand of multiband personal communications handsets fosters development of small-size integrated multiband antennas. Microstrip antennas appeared as a by-product of microstrip circuits, which by then had become a mature technology. Their design and realization took advantage of the techniques developed for microstrip circuits and used microstrip circuit substrates. The preferred solutions are usually metallic patches with multiple resonances. These Patches allow a great flexibility in the antenna design, as they are cost–effective and straight forward to produce, as well as easy to adapt to the shape of the handset.

The demand for high performance multi-standard communication handsets has led to the research and studies of this interesting topic. Therefore, it is important to study the basic concepts of multiband antenna systems, a system that brings the world of wireless communication to a new era.

The first leap to understanding multiband microstrip patch antenna systems lead to the fundamental studies on antenna theory and their design parameters. Laying a good foundation is essential. The radiation patterns and input return loss of the multiband microstrip patch antennas at different resonant frequencies will have to be investigated and thus, further research will be carried out to bring a better insight by simulation methods. The area of study will conclude with analysis on simulations for the multiband microstrip antenna system. Hence, our aim is to design a multiband triangular patch antenna and also to reduce the return loss of the antenna so that more power will enter in the antenna & high efficiency is achieved.

1.2 Motivation & Objective

Microstrip patch antennas are popular for wireless application due to their low-profile structure. Therefore these antennas are extremely compatible for embedded in handheld wireless devices such as cellular phones, pagers etc. The telemetry communication antennas on missiles need to be thin and conformal and are often Microstrip patch antennas.

The increasing demand of microstrip patch antenna has made to focus towards the study of rectangular and triangular patch and fractal antenna. Work in the thesis is to study the patch & fractal antenna, and also to design the rectangular patch and triangular patch antenna operating at 2.4 GHz for Wi-Fi application.

1.3 Thesis Organisation

The thesis report is divided into seven chapters, each having ample information for comprehending the concepts of this project.

Chapter 1 provides the introduction of the work and motivation also discuss the objective of the project.

Chapter 2 introduces the antenna and also describing the fundamental antenna parameters and makes a brief description of microstrip antennas in this chapter.

Chapter 3 provide the detail of the microstrip antennas, for example its working principle and design techniques, analysis of microstrip antennas, feeding techniques and linearly polarized microstrip antennas will be dealt with.

Chapter 4 discusses the Triangular patch antenna & their design.

Chapter 5 deals with the basics of the fractal antennas.

Chapter 6 discuss the results & simulation of the rectangular, triangular & fractal antennas & also provide comparison among various results.

Chapter 7 draws a summary and concludes the thesis with future scope.

Chapter 2

Antenna

2.1. Antennas

Communications has become the key to momentous changes in the organization of businesses and industries as they themselves adjust to the shift to an information economy. Information is indeed the lifeblood of modern economies and antennas provide mother earth a solution to a wireless communication system [5].

The radio antenna is an essential component in any radio system. An antenna is a device that provides a means for radiating or receiving radio waves. In other words, it provides a transition from guided waves on a transmission line to a “free space” wave (and vice versa in the receiving case). Thus information can be transferred between different locations without any intervening structure. Furthermore, antennas are required in situations where it is impossible, impractical or uneconomical to provide guiding structures between the transmitter and the receiver. A guided wave traveling along a transmission line, which opens out as in figure 2.1, will radiate as free space wave. The guided wave is a plane wave while the free space wave is an spherically expanding wave [1]. Along the uniform part of the line, energy is guided, as a plane wave with little loss, provided the spacing between the wires is a small fraction of a wavelength. At the right, as the transmission line separation approaches a wavelength or more, the wave tends to be radiated so that the opened-out line acts like an antenna, which launched the free space wave. The currents on the transmission line flow out on the transmission line and end there, but the fields associated with them keep on going. To be more explicit, the region of transition between the guided wave and the free space wave may be defined as an antenna.

In this vast and dynamic field, the antenna technology has been an indispensable partner of the communication revolution. Many major advances that took place over the years are now in common use. Despite numerous challenges, the antenna technology has grown with a fast pace to harness the electromagnetic spectrum, which is one of the greatest gifts of nature.

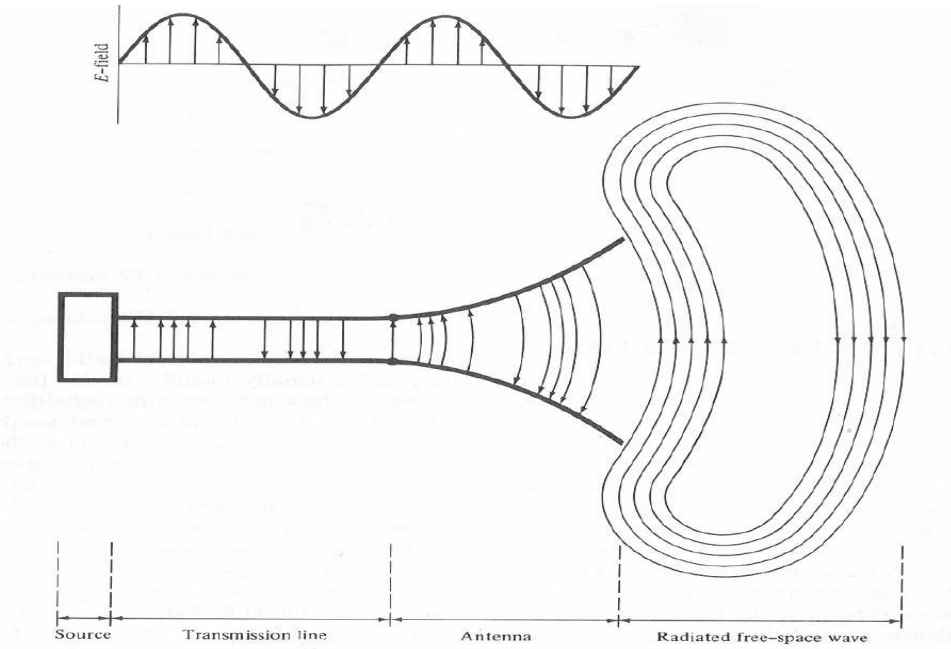

Figure .2.1: Antenna as a Transition Device

2.2. Brief Review of Maxwell's Equations

Maxwell's equations with the constitutive relations [5] are-

Differential form	Integral form
$\nabla \times E = \frac{\partial B}{\partial t}$	$\oint_c E.dl = -\int_s \frac{\partial B}{\partial t}.ds$
$\nabla \times H = J + \frac{\partial D}{\partial t}$	$\oint_c H.dl = J + \int_S (\frac{\partial D}{\partial t}).ds$
$\nabla . B = 0$	$\oint_s B.d = 0$
$\nabla . D = \rho$	$\oint_s D.ds = Q$

(2.1)

The antenna problem consists of solving the fields that are created by an impressed current distribution, **J**. In the simplest approach, this current distribution is obtained during the solution process. But, if we assume that we have the current distribution and wish to determine the fields **E** and **H**, we need only deal with the two curl equations of Maxwell's equations given above [5].

2.3. Types of Antennas

There are various types of antennas and they include wire antennas, aperture antennas, reflector antennas, lens antennas, microstrip antennas and array antennas. However, after giving a brief idea on wire antennas, aperture antennas, reflectors and lens antennas emphasis will be given to microstrip patch antennas [1].

Wire antennas: characterized by a presumed known current distribution, these are the oldest and still the most prevalent of all antenna configurations and they can be seen virtually anywhere. There are different shapes of wire antennas such as a straight wire (dipole), loop and helix.

Aperture antennas: characterized by a presumed known E-field distribution, they are most utilized for higher frequencies and antenna of this class are very useful for aircraft and space craft applications because they can easily be flush mounted onto the surface of the aircraft or space craft. Furthermore, they can be coated with a dielectric material to cushion them from hazardous conditions of the environment.

Reflector antennas are sophisticated forms of antennas used for communications over long distances. They are large in dimensions as to achieve high gain required to transmit or receive signals after millions of miles travel.

Lenses are mainly employed to collimate incident divergent energy to prevent it from spreading in undesired directions. Proper modelling of the geometrical configuration and using the correct materiel for the lenses can transform various forms of divergent energy into plane waves and these lens antennas are used in most of the applications of higher frequencies.

2.4. Basic Antenna Parameters

Definitions of various parameters are necessary to describe the performance of an antenna. Although the parameters may be interrelated, it is however, not a requirement to specify all the parameters for complete description of the antenna performance. An antenna is chosen for operation in a particular application according to its physical and electrical characteristics. Furthermore, the antenna must perform in a required mode for

the particular measurement system. An antenna can be characterized by the following parameters, not all of which apply to all antenna types [1].

1. Radiation pattern
2. Radiation resistance
3. Beam width and gain of main lobe.
4. Position and magnitude of side lobes.
5. Magnitude of back lobe.
6. Bandwidth
7. Aperture
8. Antenna correction factor
9. Polarization of the electric field that it transmits or receives
10. Power that the antenna can handle
11. Efficiency

Typically, antenna characteristics are measured in two principal planes and they are known as azimuth and elevation planes, which can also be considered as the horizontal and vertical planes. Conventionally, the angle in the azimuth plane is denoted by the Greek letter phi (Φ) while the Greek letter theta (θ) represents the angle in the elevation plane. Not all of the antenna characteristic factors will be discussed here. The following subsection will touch on some of the antenna parameters, which are essential for the understanding of the thesis.

2.4.1. Radiation Pattern

The antenna, which radiates or receives the electromagnetic energy in the same way, is a reciprocal device. Radiation pattern is very important characteristic of an antenna. It facilitates a stronger understanding of the key features of an antenna that otherwise cannot be achieved from the textual technical description of an antenna. A radiation pattern (antenna pattern) is a graphical representation of the radiations (far-field) properties of an antenna. To completely specify the radiation pattern with respect to field intensity and polarization, three patterns are required [1].

1. The θ component of the electric field as a function of the angles θ and Φ or $E_\theta(\theta,\Phi)$. (Volt/meter)
2. The Φ component of the electric field as a function of the angles θ and Φ or $E_\Phi(\theta,\Phi)$. (Volt/meter)
3. The phases of these fields as a function of the angles θ and Φ or $\delta_\theta(\theta,\Phi)$ and $\delta_\Phi(\theta,\Phi)$. (degree or radian)

Although the radiation characteristics of an antenna involve three-dimensional patterns, many important radiation characteristics can be expressed in terms of simple single valued scalar quantities. These include-

-Beamwidths, beam area, main-lobe beam area and beam efficiency; directivity and gain

-Effective aperture, scattering aperture, aperture efficiency and effective height. The radiation pattern can be plotted using rectangular/Cartesian or polar coordinates. The rectangular plots can be read more precisely (since the angular scale can be enlarged), but the polar plots offer a more pictorial representation and are thus easier to visualize.

2.4.1.1 Rectangular /Cartesian Plots

Rectangular /Cartesian plots are standard x-y plots where the axes are plotted at right angle to each other. In a radiation plot, the angle with respect to bore sight is varied and the magnitude of the power radiated is measured; thus the angle is the independent variable and the power radiated is the dependent variable, A typical rectangular plot of an antenna radiation pattern is shown in Fig.2.2.

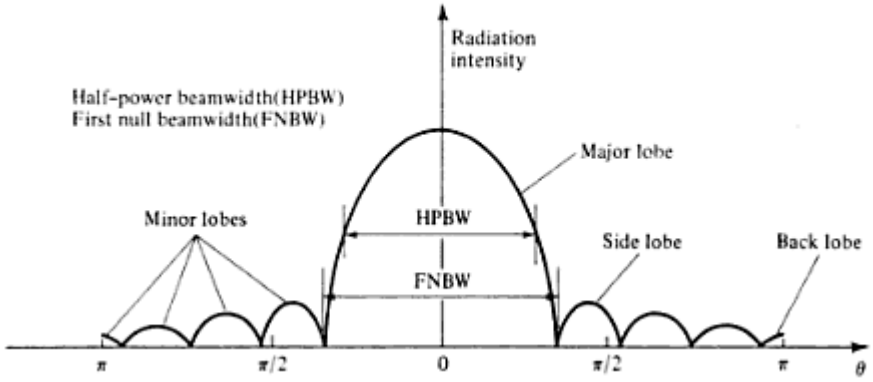

Figure.2.2: Rectangular Plot of an Antenna Pattern [1]

2.4.1.2. Polar Plots

In polar plot, the angles are plotted radially from bore sight and the power or intensity is plotted along the radius as shown in figure 2.3.

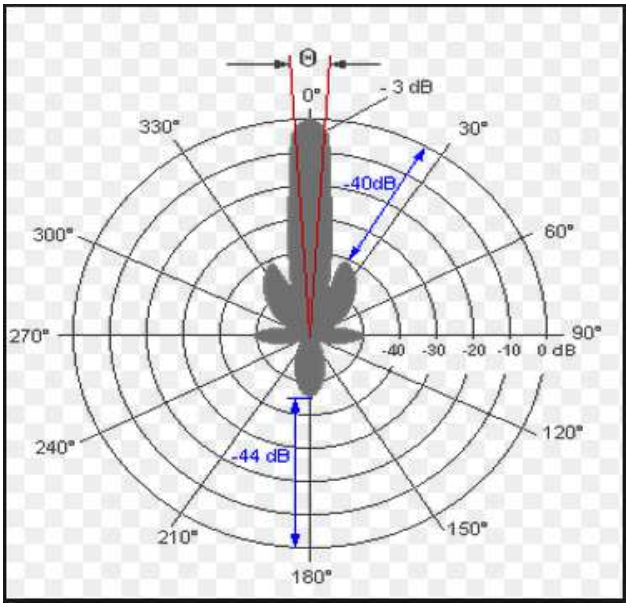

Figure 2.3 -typical polar plot of an antenna [1]

This gives a pictorial representation of radiation pattern of the antenna and is easier to visualize than the rectangular/Cartesian plots. Although the accuracy cannot be increased as in the case of rectangular plot because the scale of the angular positions can only be plotted from 0^0 to 360^0, however, the scale of the intensity of power can be varied. Each circle on the polar plot represents a contour plot where the power has the same magnitude and is shown relative to the power at bore sight. These levels will always be less than the power at bore sight and values should be shown as negative because the power in general is maximum at bore sight. However, they are normally written without a sign and should be assumed to be negative, contrary to standard arithmetic convention.

2.4.2. Half-Power Beam Width

The half-power beamwidth is defined as: “In a plane containing the direction of the maximum of a beam, the angle between the two directions in which the radiation intensity is one-half the maximum value of the beam.” Often the term beamwidth is

used to describe the angle between any two points on the pattern such as the angle between the 10-dB points [5].

The beam width of the antenna is a very important figure of merit, and it often used as a trade-off between the bandwidth and the side lobe level; that is, as the bandwidth decreases the side lobe increases and via versa [1].

2.4.3 Beam Efficiency

Beam efficiency is another parameter that is frequently used to judge the quality of transmitting and receiving antennas. For an antenna with its major lobe directed along the z-axis (θ=0 degree), the beam efficiency (BE) is defined as.

$$\text{BE} = \frac{\text{power transmitted (received) within cone angle } \theta_1}{\text{power transmitted (received) by the antenna}} \tag{2.2}$$

Where θ is the half-angle of the cone with in which the percentage of the total power is to be found.

$$BE = \frac{\int_0^{2\Pi}\int_0^{\theta_1} U(\theta,\phi)\sin\theta d\theta d\phi}{\int_0^{2\Pi}\int_0^{\Pi} U(\theta,\phi)\sin\theta d\theta d\phi} \tag{2.3}$$

If θ_1 is chosen as the angle where the first null or minimum occurs , then the beam efficiency will indicate the amount of power in the major lobe compared to the total power , a very high beam efficiency usually in the high 90s , is necessary for antennas used in radiometry , astronomy , radar and other applications where received signals through the minor lobes must be minimized.

2.4.4. Bandwidth

The Bandwidth of an antenna is defined as “the range of frequencies within which the performance of the antenna, with respect to some characteristics, conforms to a specified standard”. The bandwidth can be considered to be the range of frequencies, on either side of a centre frequency (usually the resonance frequency for a dipole), where the antenna characteristics (such as input impedance, pattern, beam width, polarization, side lobe level, gain, beam direction, beamwidth , radiation efficiency) are within an acceptable value of those at the centre frequency.

For narrow band antennas, the bandwidth is expressed as a percentage of the frequency difference (upper minus lower) over the centre frequency of the bandwidth [1].

2.4.5. Polarization

Polarization of an antenna in a given direction is defined as “the polarization of the wave radiated by the antenna. Note: when the direction is not stated, the polarization is taken to be the polarization in the direction of maximum gain.” Polarization of a radiated wave is defined as “that property of an electromagnetic wave describing the time varying direction and relative magnitude of the electric field vector specifically, the figure traced as a function of time by the extremity of the vector at a fixed location in space, and the sense in which it is traced, as observed along the direction of propagation.” Polarization then is the curve traced, by the end point of the arrow representing the instantaneous electric field [1]. A typical trace as a function of time is shown in figure 2.4.

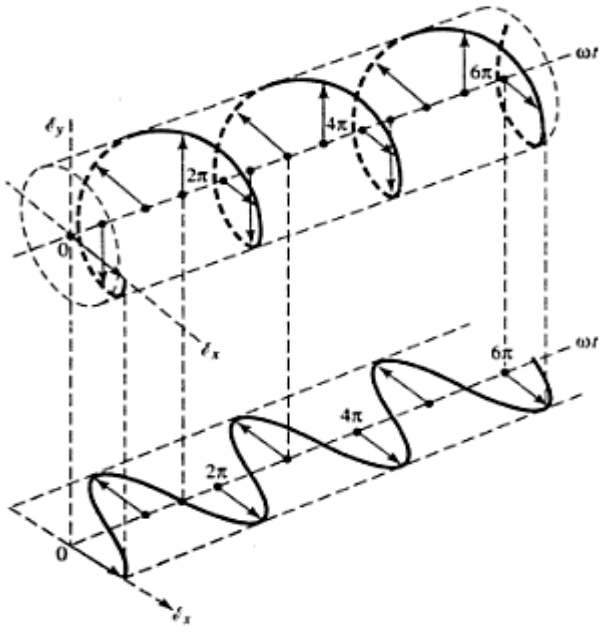

(a) Rotation of wave.

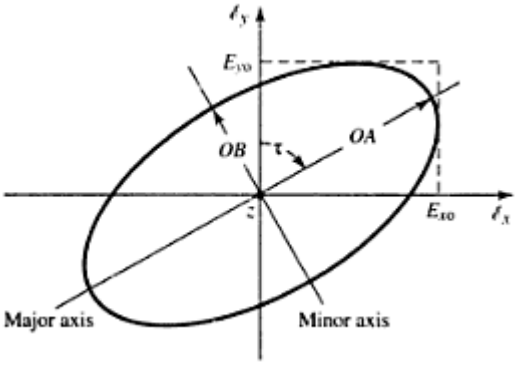

(b) Polarization ellipse.

Figure 2.4. Rotation of a Plane Electromagnetic Wave and its Polarization Ellipse at z=0 as a function of time.

Polarization may be classified as linear, circular, or elliptical. If the vector that describes the electric field at a point in space as a function of time is always directed along a line, the field is said to be linearly polarized. In general, however, the figure that the electric field traces is an ellipse and the field is said to be elliptically polarized [1]. Linear and circular polarizations are special cases of elliptical, and they can be obtained when the ellipse becomes a straight line or a circle respectively.

The rotation of the electric field vector is traced in clockwise (cw) or counter clockwise (ccw) sense. Clockwise rotation of the electric field vector is designated as right hand polarization and counter clockwise as left hand polarization.

2.4.6. Directivity, Gain, and Beam Width

The directive gain of an antenna system towards a given direction (θ,Φ) is the radiation Intensity normalized by the corresponding isotropic intensity, that is [12]

$$D(\theta,\phi)=\frac{U(\theta,\phi)}{U_I} \qquad (2.4)$$

Where U (θ,Φ) is the radiation intensity, which is defined to be the power radiated per unit solid angle of the antenna system under consideration, and UI is the radiation intensity of an isotropic antenna. The directive gain measures the ability of the antenna to direct its power towards a given direction. The maximum value of the directive gain, D_{max}, is called the directivity of the antenna and will be realized towards some particular

direction, say (θ_O,Φ_O). The radiation intensity will be maximum towards that direction, U_{max} = U (θ_0, Φ_0), so that

$$D_{\max} = \frac{U_{\max}}{U_I} \tag{2.5}$$

Another useful concept is that of the beam solid angle of an antenna. The definition is motivated by the case of a highly directive antenna, which concentrates all of its radiated power into a small solid angle $\Delta\Omega$ [12].

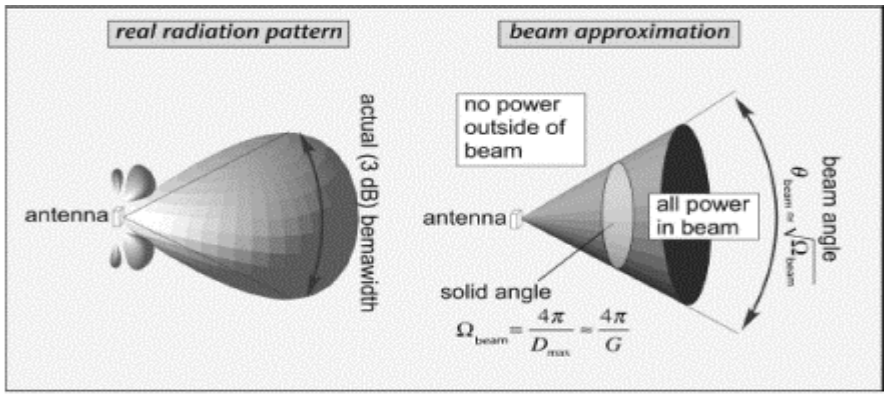

Figure 2.5. Beam approximation for the radiation pattern of directional antenna.

The radiation intensity in the direction of the solid angle will be:

$$U = \frac{P_{rad}}{\Delta\Omega} \tag{2.6}$$

It follows that:

$$D_{\max} = \frac{4\Pi U}{P_{rad}} = \frac{4\Pi}{\Delta\Omega} \tag{2.7}$$

2.5. Theory of Small Antennas

The small antennas studied in this thesis are resonators. Because a small antenna stores a relatively large amount of energy, its input impedance has a large reactive component in addition to a small radiation resistance. To deliver power to (and from) the antenna, it must be tuned to resonance, i.e. the input reactance must be cancelled out. Sufficient reactance cancellation can only occur inside a narrow bandwidth. In addition, the resonant resistance must be transformed to match the characteristic impedance of the feed line. A small antenna can be tuned to resonate with an appropriate additional

reactance, or it can be made to self-resonate so that the reactance cancellation at resonance happens naturally in the antenna structure.

In the following, some theory of electrically small antennas is briefly discussed. The purpose is to define the most important terms and to explain what will happen when the antenna size is reduced, since miniaturization is the key word for the antenna designer of this wireless era.

2.5.1. Quality Factor

The quality factor of a resonator describes the rate at which energy decays in the resonator [13]. It is defined as

$$Q = \frac{\omega_r \text{ x energy stored in the resonator}}{\text{decrease of energy per second}} = 2\pi f_r \frac{W}{P_l} \qquad (2.8)$$

Where ω_r is angular resonant frequency, f_r is resonant frequency, w is stored energy, and P_l is power loss. At the resonant frequency, the electric and magnetic energies of the resonator are equal. The loss power can be divided into several load components, each of which can be described with a separate quality factors. The total quality factor is called the loaded quality factor (Q_l). It can be divided into the unloaded quality factor (Q_o) and the external quality factor (Q_e), as shown by equation (2.8). The unloaded quality factor describes the internal losses of the resonator, which can be further divided into radiation, conductor, and dielectric losses. These are described by radiation (Q_r), conductor (Q_c), and dielectric (Q_d) quality factors respectively. One or more external quality factors can be used to describe the losses caused by external connections to the resonator, such as the antenna feed [13].

$$\frac{1}{Q_l} = \frac{1}{Q_o} + \frac{1}{Q_e} = \frac{1}{Q_r} + \frac{1}{Q_d} + \frac{1}{Q_e} \qquad (2.9)$$

The unloaded quality factor of a resonator can be determined from a simulated or measured frequency response of reflection coefficient

2.5.2. Bandwidth

The useful bandwidth of an antenna may be limited by several factors, such as impedance, gain, polarization, or beamwidth. The input impedance is generally the main factor limiting the usable bandwidth of small antennas. The input impedance of a small antenna varies rapidly with frequency. This limits the frequency range over which the antenna can be matched to its feed line.

Impedance bandwidth is usually specified in terms of a return loss (Lrten) or voltage standing wave ratio (*VSWR*). Typical matching requirements are VSWR≤ 2 or Lretn ≥ 10 dB [1]. Usually, the matching requirement is set in each case separately to meet the requirements of the application at hand. In recent years, Lretn ≥ 6dB(*VSWR* ≤ 3) has become a typical requirement for small internal antennas of mobile phones .Near resonance, the input impedance of a small antenna can be modelled by a parallel or series Resistance-Inductance-Capacitance(RLC) lumped-element equivalent circuit. By using a resonant circuit model, it can be shown that the relative impedance bandwidth Br of a small antenna is inversely proportional to its unloaded quality factor.

$$B_r = \frac{1}{Q_0}\sqrt{\frac{(TS-1)(S-T)}{S}} \qquad (2.10)$$

2.5.3. Minimum Radiation Quality Factor of a Small Antenna

The minimum radiation quality factor and the maximum bandwidth of an ideal single resonant small antenna are ultimately limited by the antenna size. The fields outside a virtual sphere (radius a), which completely encloses an antenna structure or an arbitrary current distribution, can be expressed with a complete set of orthogonal, spherical wave functions (spherical TM_{mn} and TE_{mn} wave modes). The space outside the virtual sphere can be thought of as a spherical wave-guide where the waves propagate in the radial direction. The cutoff radius of the spherical wave-guide is $r_c=n\lambda_o/2\pi$, where n is the mode number. The cutoff radius is independent of the mode number n. All the modes excited by the antenna contribute to the reactive power while only the propagating modes contribute to the radiated power. When the sphere around the antenna decreases, the number of propagating modes decreases and Qr increases. When the sphere becomes small enough, even the lowest mode (n=1) becomes evanescent (non-propagating), and Qr increases rapidly, as evanescent modes contribute very little to the radiated power. With the use of the spherical wave modes, it is shown that of all

linearly polarized small antennas, the lowest possible Qr is obtained with an antenna that excites only either one of the lowest modes (TM_{01} or TE_{01}) outside the enclosing virtual sphere and stores no energy inside it. The theoretical minimum Qr of such an antenna can be calculated from

$$Q_r = \frac{1}{(ka)^3} + \frac{1}{ka} \qquad (2.11)$$

Where k is wave number ($k = 2\pi/\lambda o$), and a is the radius of the smallest sphere enclosing the antenna. In practice, however, all the antennas store energy also within the enclosing sphere, which increases their Qr. Thus, equation (2.10) represents a fundamental lower limit, which is not reached with practical linearly polarized antennas. According to equation (2.10), the radiation quality factor of an ideal small antenna is approximately inversely proportional to the volume of the antenna in wavelengths ($V/\lambda o^3$). Based on the spherical wave mode theory, practical small antennas such as shorted patches, must behave qualitatively the same way as the ideal antenna. The radiation quality factors of practical antennas are just higher, as explained above. When both TM01 and TE01 modes are equally excited, as in circularly polarized small antennas, the theoretical minimum Qr is about half of that obtained when only TM01 or TE01 mode is excited. The theoretical minimum Qr of an ideal small antenna, with TM01 and TE01 modes equally excited, can be calculated from

$$Q_r = \frac{1}{2(ka)^3} + \frac{1}{ka} \qquad (2.12)$$

Generally, to minimize Qr, the antenna structure should use the space inside the enclosing sphere as efficiently as possible. For example, the Qr of the PIFA is known to decrease as its height increases. The height of a basic PIFA can be increased without increasing the radius of the enclosing sphere, because the condition for its fundamental resonance is related to its length (l) and height (h) as $l + h = \lambda/4$. Therefore, it can be argued that increasing the height of a PIFA makes its Qr approach the theoretical limit because the antenna utilizes the volume of the enclosing sphere more efficiently.

2.5.4. Efficiency

Total antenna efficiency (η_t) measures how well an antenna converts the input power available at the antenna feed to radiated power (P_r), which can be measured in the far field. The total efficiency can be divided into radiation efficiency (η_r) and reflection (mismatch) efficiency (η_{reff}).

$$\eta_t=\eta_r\ \eta_{reff} \quad (2.13)$$

Radiation efficiency tells how much of the input power accepted by an antenna (Pin) it converts to radiated power. Radiation efficiency can also be expressed as the ratio of the unloaded quality factor to the radiation quality factor of the antenna. As shown by equations (2.8) and (2.9), if Q_r increases, Q_c and Q_d must be increased accordingly, otherwise the radiation efficiency decreases. For a given radiation efficiency, a narrowband antenna requires the use of less lossy materials than a wideband antenna.

$$\eta_t =P_r/P_{in}= Q_o/Q_r \quad (2.14)$$

Proper matching ensures that a desired amount of the available power is transferred into the antenna. Reflection efficiency is defined as

$$\eta_{erfl}=1- |\Gamma|^2 \quad (2.15)$$

Where Γ is voltage reflection coefficient at the antenna feed. It can be calculated from

$$\Gamma=(Z_{in}-Z_o)/(Z_{in}+Z_o) \quad (2.16)$$

Where Zin is antenna input impedance, and Z_0 is characteristic impedance of the feed line The typical radiation quality factors of the antennas studied in this thesis are small enough and the materials are so good (Qc and Qd sufficiently high) that the radiation efficiency is not the main factor limiting the total efficiency of the antennas. The total efficiency is mainly limited by the reflection efficiency at the edges of the operation band.

Chapter 3

Patch Antenna

In this chapter, an introduction to the Microstrip Patch Antenna is followed by its advantages and disadvantages. Next, some feed modelling techniques are discussed. Finally, a detailed explanation of Microstrip patch antenna analysis and its theory are discussed, and also the working mechanism is explained.

3.1 Introduction

In its most basic form, a Microstrip patch antenna consists of a radiating patch on one side of a dielectric substrate which has a ground plane on the other side as shown in Figure 3.1. The patch is generally made of conducting material such as copper or gold and can take any possible shape. The radiating patch and the feed lines are usually photo etched on the dielectric substrate.

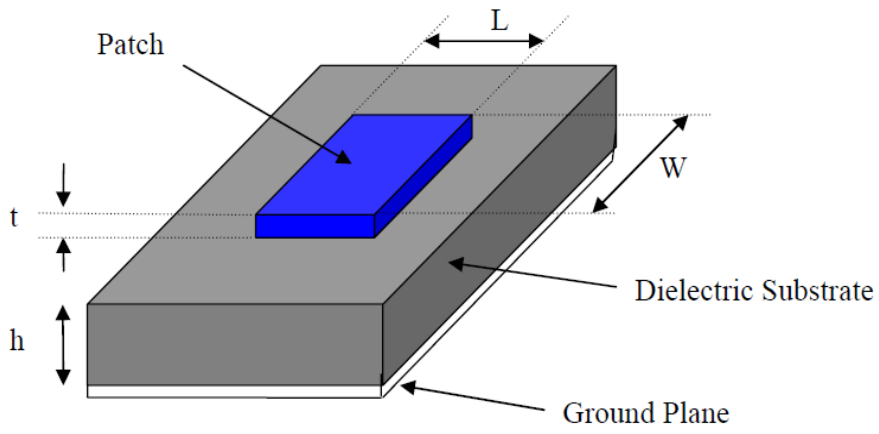

Figure 3.1 Structure of a Microstrip Patch Antenna

In order to simplify analysis and performance prediction, the patch is generally square, rectangular, circular, triangular, elliptical or some other common shape as shown in Figure 3.2. For a rectangular patch, the length L of the patch is usually $0.3333\lambda < L < 0.5\lambda$, where λ_O is the free-space wavelength. The patch is selected to be very thin such that $t << \lambda$ (where t is the patch thickness). The height h of the dielectric substrate is

usually $0.003\ \lambda_O \leq h \leq 0.05\lambda_O$. The dielectric constant of the substrate (ε_r) is typically in the range $2.2 \leq \varepsilon r \leq 12$.

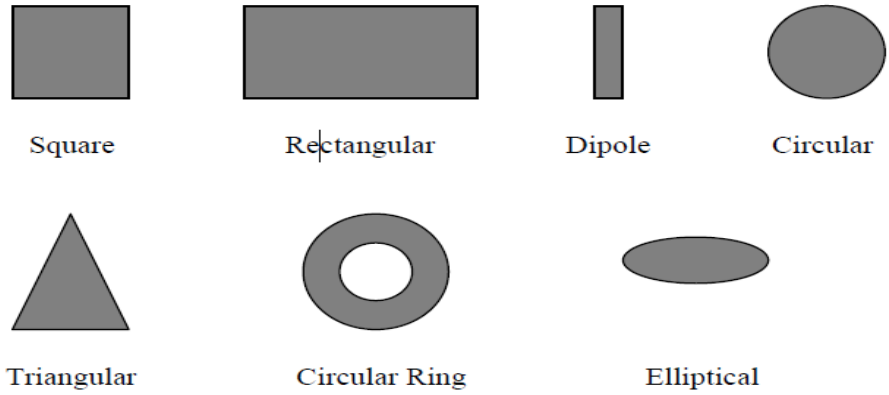

Figure 3.2 Common shapes of microstrip patch elements

Microstrip patch antennas radiate primarily because of the fringing fields between the patch edge and the ground plane. For good antenna performance, a thick dielectric substrate having a low dielectric constant is desirable since this provides better efficiency, larger bandwidth and better radiation [1]. However, such a configuration leads to a larger antenna size. In order to design a compact Microstrip patch antenna, higher dielectric constants must be used which are less efficient and result in narrower bandwidth. Hence a compromise must be reached between antenna dimensions and antenna performance.

3.2. Microstrip Structures

A microstrip structure is made with a thin sheet of low-loss insulating material called the dielectric substrate. It is completely covered with metal on one side, called the ground plane, and partly metallized on the other side, where the circuit or antenna shapes are printed [7]. Components can be included in the circuit either by implanting lumped components (resistors, inductors, capacitors, semiconductors, and ferrite devices) or by realizing them directly with in the circuit. Each part of the microstrip structure will be explained in detail as follows.

3.2.1. Dielectric Substrate

The Dielectric substrate is the mechanical backbone of the microstrip circuit. It provides a stable support for the conductor strips and patches that make up connecting lines, resonators and antennas. It ensures that the components that are implanted are properly located and firmly held in place, just as in printed circuits for electronics at lower frequencies.

The substrate also fulfils an electrical function by concentrating the electromagnetic fields and preventing unwanted radiation in circuits. The dielectric is an integral part of the connecting transmission lines and deposited components: its permittivity and thickness determine the electrical characteristics of the circuit or of the antenna.

3.2.2. Conductor Layers

Nowadays, many commercial suppliers provide a wide range of microstrip substrates, already metallized on both faces. The conductor on the upper face is chemically etched to realize the circuit pattern by a photographic technique. A mask of the circuit of the antenna is drawn, generally at convenient scale, and then reduced and placed in close contact with a photo resistive layer, which was previously deposited on top of the metallized substrate. The lower metal part is the ground plane. The ground plane, besides acting as a mechanical support, provides for integration of several components and serves also as a heat sink and dc bias return for active devices. The resulting sandwich is then exposed to ultraviolet rays, which reach the photosensitive layer where it is not covered by the mask. The exposed parts are removed by the photographic development, and the metal cover is etched away from the exposed area. This process is called the subtractive process.

Alternately, one may wish to use a bare dielectric substrate as a starting material and deposit metal either by evaporation or by sputtering through the holes in the mask. This is called the additive thin-film process. In the thick-film process, a metallic paste is squeezed through the holes in a mask deposited over a silk screen. The latter approach, however, is less accurate and is seldom used at very high frequencies.

3.3 Advantages and Disadvantages

Microstrip patch antennas are increasing in popularity for use in wireless applications due to their low-profile structure. Therefore they are extremely compatible for embedded antennas in handheld wireless devices such as cellular phones, pagers etc. The telemetry communication antennas on missiles need to be thin and conformal and are often Microstrip patch antennas. Another area where they have been used successfully is in Satellite communication. Some of their principal advantages discussed by [1] and Kumar and Ray [9] are given below:

• Light weight and low volume.
• Low profile planar configuration which can be easily made conformal to host surface.
• Low fabrication cost, hence can be manufactured in large quantities.
• Supports both, linear as well as circular polarization.
• Can be easily integrated with microwave integrated circuits (MICs).
• Capable of dual and triple frequency operations.
• Mechanically robust when mounted on rigid surfaces.

Microstrip patch antennas suffer from a number of disadvantages as compared to conventional antennas. Some of their major disadvantages discussed by [9] and Garg et al [10] are given below:
• Narrow bandwidth
• Low efficiency
• Low Gain
• Extraneous radiation from feeds and junctions
• Poor end fire radiator except tapered slot antennas
• Low power handling capacity.
• Surface wave excitation

Microstrip patch antennas have a very high antenna quality factor (Q). Q represents the losses associated with the antenna and a large Q leads to narrow bandwidth and low efficiency. Q can be reduced by increasing the thickness of the dielectric substrate. But as the thickness increases, an increasing fraction of the total power delivered by the source goes into a surface wave. This surface wave contribution can be counted as an

unwanted power loss since it is ultimately scattered at the dielectric bends and causes degradation of the antenna characteristics. However, surface waves can be minimized by use of photonic band gap structures as discussed by Qian et al [11]. Other problems such as lower gain and lower power handling capacity can be overcome by using an array configuration for the elements.

3.4 Feed Techniques

Microstrip patch antennas can be fed by a variety of methods. These methods can be classified into two categories- contacting and non-contacting. In the contacting method, the RF power is fed directly to the radiating patch using a connecting element such as a microstrip line. In the non-contacting scheme, electromagnetic field coupling is done to transfer power between the microstrip line and the radiating patch [1]. The four most popular feed techniques used are the microstrip line, coaxial probe (both contacting schemes), aperture coupling and proximity coupling (both non-contacting schemes).

3.4.1 Microstrip Line Feed

In this type of feed technique, a conducting strip is connected directly to the edge of the microstrip patch as shown in Figure 3.3. The conducting strip is smaller in width as compared to the patch and this kind of feed arrangement has the advantage that the feed can be etched on the same substrate to provide a planar structure.

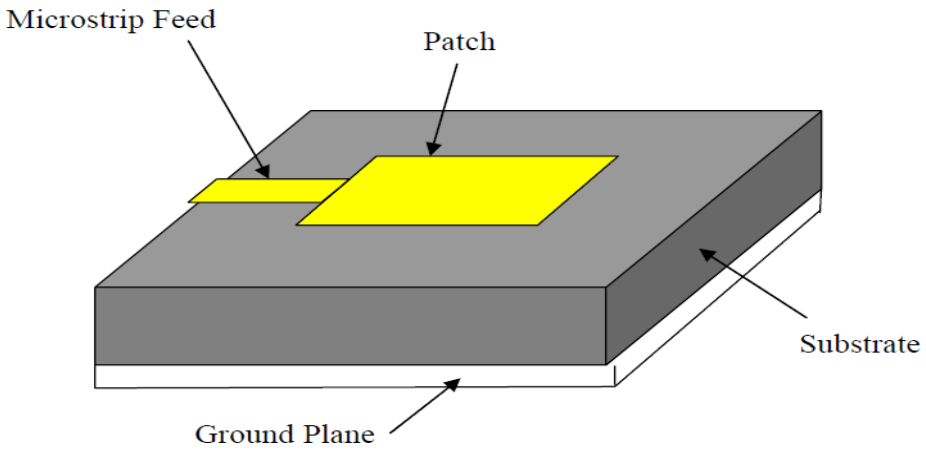

Figure 3.3 Microstrip Line Feed

The purpose of the inset cut in the patch is to match the impedance of the feed line to the patch without the need for any additional matching element. This is achieved by properly controlling the inset position. Hence this is an easy feeding scheme, since it provides ease of fabrication and simplicity in modelling as well as impedance matching. However as the thickness of the dielectric substrate being used, increases, surface waves and spurious feed radiation also increases, which hampers the bandwidth of the antenna [1]. The feed radiation also leads to undesired cross polarized radiation.

3.4.2 Coaxial Feed

The Coaxial feed or probe feed is a very common technique used for feeding Microstrip patch antennas. As seen from Figure 3.4, the inner conductor of the coaxial connector extends through the dielectric and is soldered to the radiating patch, while the outer conductor is connected to the ground plane.

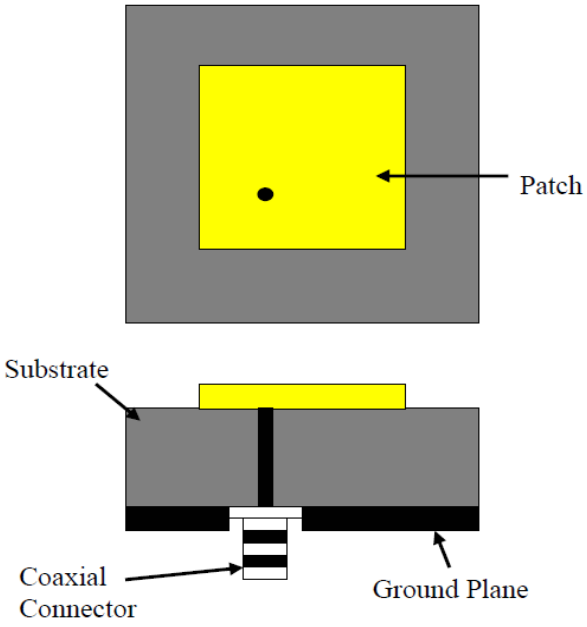

Figure 3.4 Probe fed Rectangular Microstrip Patch Antenna

The main advantage of this type of feeding scheme is that the feed can be placed at any desired location inside the patch in order to match with its input impedance. This feed method is easy to fabricate and has low spurious radiation. However, its major disadvantage is that it provides narrow bandwidth and is difficult to model since a hole

has to be drilled in the substrate and the connector protrudes outside the ground plane, thus not making it completely planar for thick substrates ($h > 0.02\lambda o$). Also, for thicker substrates, the increased probe length makes the input impedance more inductive, leading to matching problems [9]. This problem has been solved by the non-contacting feed techniques which have been discussed below.

3.4.3 Aperture Coupled Feed

In this type of feed technique, the radiating patch and the microstrip feed line are separated by the ground plane as shown in Figure 3.5. Coupling between the patch and the feed line is made through a slot or an aperture in the ground plane.

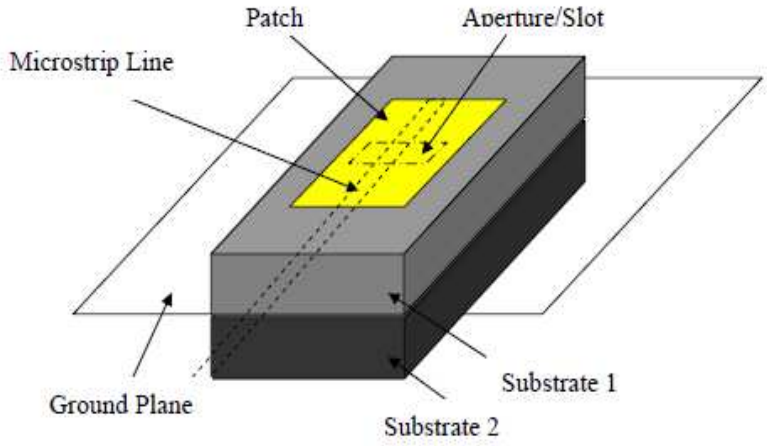

Figure 3.5 Aperture-coupled feed

The coupling aperture is usually centred under the patch, leading to lower cross polarization due to symmetry of the configuration. The amount of coupling from the feed line to the patch is determined by the shape, size and location of the aperture. Since the ground plane separates the patch and the feed line, spurious radiation is minimized. Generally, a high dielectric material is used for the bottom substrate and a thick, low dielectric constant material is used for the top substrate to optimize radiation from the patch [1]. The major disadvantage of this feed technique is that it is difficult to fabricate due to multiple layers, which also increases the antenna thickness. This feeding scheme also provides narrow bandwidth.

3.4.4 Proximity Coupled Feed

This type of feed technique is also called as the electromagnetic coupling scheme. As shown in Figure 3.6, two dielectric substrates are used such that the feed line is between the two substrates and the radiating patch is on top of the upper substrate. The main advantage of this feed technique is that it eliminates spurious feed radiation and provides very high bandwidth (as high as 13%) [1], due to overall increase in the thickness of the microstrip patch antenna. This scheme also provides choices between two different dielectric media, one for the patch and one for the feed line to optimize the individual performances.

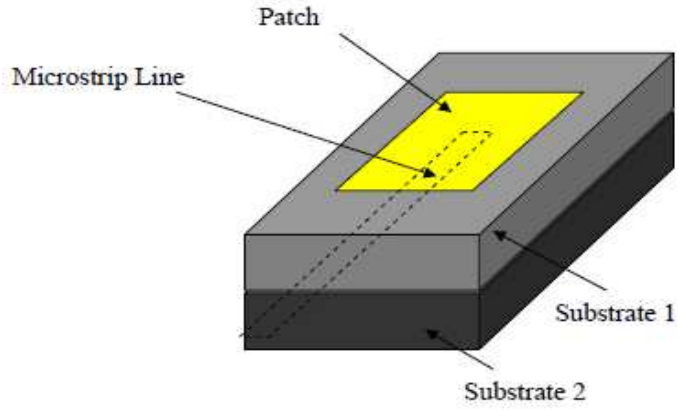

Figure 3.6 Proximity-coupled Feed

Matching can be achieved by controlling the length of the feed line and the width-to-line ratio of the patch. The major disadvantage of this feed scheme is that it is difficult to fabricate because of the two dielectric layers which need proper alignment. Also, there is an increase in the overall thickness of the antenna.

Table 3.1 summarizes the characteristics of the different feed techniques.

Characteristics	Microstrip Line Feed	Coaxial Feed	Aperture coupled Feed	Proximity coupled Feed
Spurious feed radiation	More	More	Less	Minimum
Reliability	Better	Poor due to soldering	Good	Good
Ease of fabrication	Easy	Soldering and drilling needed	Alignment required	Alignment required
Impedance Matching	Easy	Easy	Easy	Easy
Bandwidth (achieved with impedance matching)	2-5%	2-5%	2-5%	13%

Table 3.1 Comparison between the different feed techniques [4].

3.5 Methods of Analysis

The most popular models for the analysis of Microstrip patch antennas are the transmission line model, cavity model, and full wave model [1] (which include primarily integral equations / Moment Method). The transmission line model is the simplest of all and it gives good physical insight but it is less accurate. The cavity model is more accurate and gives good physical insight but is complex in nature. The full wave models are extremely accurate, versatile and can treat single elements, finite and infinite arrays, stacked elements, arbitrary shaped elements and coupling. These give less insight as compared to the two models mentioned above and are far more complex in nature.

3.5.1 Transmission Line Model

This model represents the microstrip antenna by two slots of width *W* and height h, separated by a transmission line of length L. The microstrip is essentially a non homogeneous line of two dielectrics, typically the substrate and air.

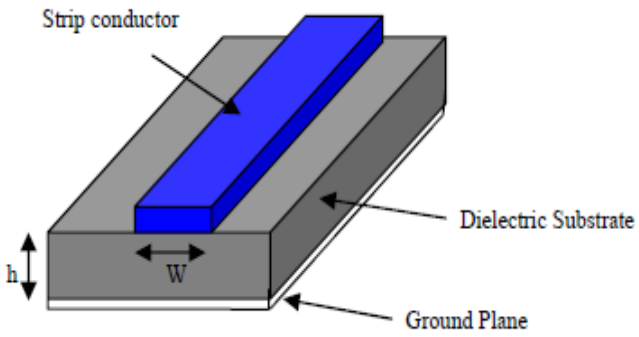

Figure 3.7 Microstrip Line

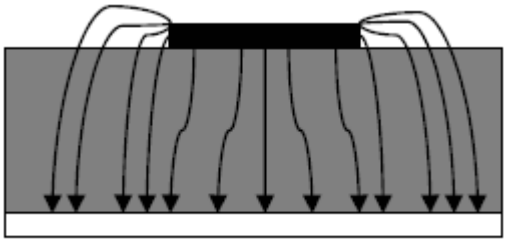

Figure 3.8 Electric Field Lines

Hence, as seen from Figure 3.8, most of the electric field lines reside in the substrate and parts of some lines in air. As a result, this transmission line cannot support pure transverse electric-

Magnetic (TEM) mode of transmission, since the phase velocities would be different in the air and the substrate. Instead, the dominant mode of propagation would be the quasi-TEM mode. Hence, an effective dielectric constant (ε_{eff}) must be obtained in order to account for the fringing and the wave propagation in the line. The value of ε_{eff} is slightly less then ε_r because the fringing fields around the periphery of the patch are not confined in the dielectric substrate but are also spread in the air as shown in Figure 2.8 above. The expression for ε_{eff} is given by Balanis [3] as

$$\varepsilon_{reff} = \frac{\varepsilon_r + 1}{2} + \frac{\varepsilon_r - 1}{2}\left[1 + 12\frac{h}{W}\right]^{-\frac{1}{2}} \tag{3.1}$$

Where ε_{reff} = Effective dielectric constant

ε_r = Dielectric constant of substrate

h = Height of dielectric substrate

W = Width of the patch

Consider Figure 3.9 below, which shows a rectangular microstrip patch antenna of length *L*, width *W* resting on a substrate of height *h* . The co-ordinate axis is selected such that the length is along the *x* direction, width is along the *y* direction and the height is along the *z* direction.

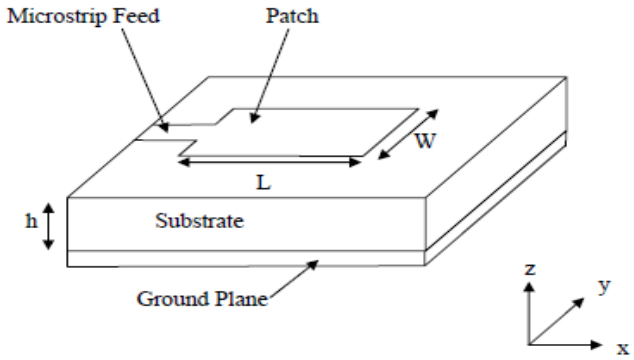

Figure 3.9 Microstrip Patch Antenna

In order to operate in the fundamental TM_{10} mode, the length of the patch must be slightly less than λ/2 where λis the wavelength in the dielectric medium and is equal to $\lambda_o/\sqrt{\varepsilon_{reff}}$ where λ*o* is the free space wavelength. The TM10 mode implies that the field varies one λ / 2 cycle along the length, and there is no variation along the width of the patch. In the Figure 3.10 shown below, the microstrip patch antenna is represented by two slots, separated by a transmission line of length L and open circuited at both the ends. Along the width of the patch, the voltage is maximum and current is minimum due to the open ends. The fields at the edges can be resolved into normal and tangential components with respect to the ground plane.

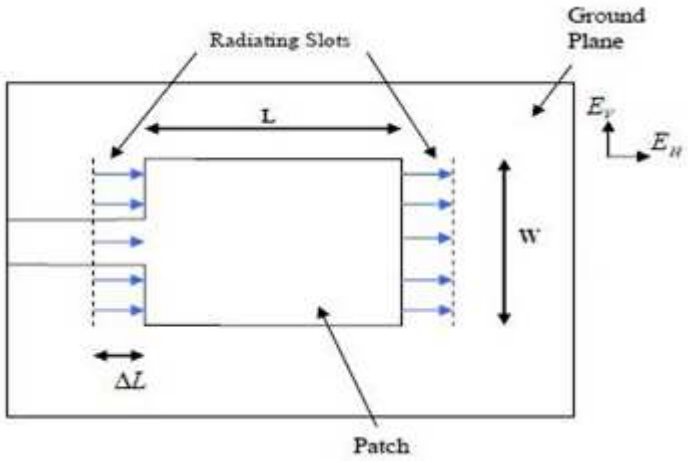

Figure 3.10 Top View of Antenna

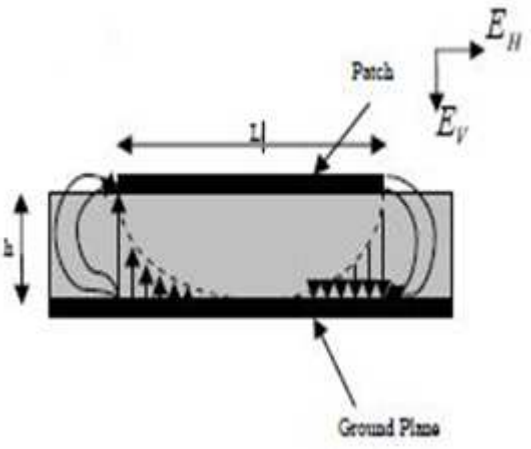

Figure 3.11 Top View of Antenna

It is seen from Figure 3.11 that the normal components of the electric field at the two edges along the width are in opposite directions and thus out of phase since the patch is λ/2 long and hence they cancel each other in the broadside direction. The tangential components (seen in Figure 3.11), which are in phase, means that the resulting fields combine to give maximum radiated field normal to the surface of the structure. Hence the edges along the width can be represented as two radiating slots, which are λ/2 apart and excited in phase and radiating in the half space above the ground plane. The fringing fields along the width can be modelled as radiating slots and electrically the patch of the microstrip antenna looks greater than its physical dimensions. The dimensions of the patch along its length have now been extended on each end by a distance ΔL , which is given empirically by Hammerstad [6] as-

$$\Delta L = 0.412h\frac{\left(\varepsilon_{reff}+0.3\right)\left(\frac{W}{h}+0.264\right)}{\left(\varepsilon_{reff}-0.258\right)\left(\frac{W}{h}+0.8\right)} \tag{3.2}$$

The effective length of the patch L_{eff} now becomes:

$$L_{\text{eff}} = \text{L} + 2\Delta\text{L} \tag{3.3}$$

For a For a given resonance frequency f_0 , the effective length is given by [9] as:

$$L_{eff} = \frac{c}{2f_o\sqrt{\varepsilon_{reff}}} \tag{3.4}$$

For a rectangular Microstrip patch antenna, the resonance frequency for any TM_{mn} mode is
given by James and Hall [14] as:

$$f_o = \frac{c}{2\sqrt{\varepsilon_{reff}}}\left[\left(\frac{m}{L}\right)^2 + \left(\frac{n}{W}\right)^2\right]^{\frac{1}{2}} \tag{3.5}$$

Where *m* and *n* are modes along *L* and *W* respectively. For efficient radiation, the width *W* is given by Bahl and Bhartia [15] as:

$$W = \frac{c}{2 f_o \sqrt{\frac{(\varepsilon_r + 1)}{2}}} \tag{3.6}$$

3.5.2 Cavity Model

Although the transmission line model discussed in the previous section is easy to use, it has some inherent disadvantages. Specifically, it is useful for patches of rectangular design and it ignores field variations along the radiating edges. These disadvantages can be overcome by using the cavity model. A brief overview of this model is given below. In this model, the interior region of the dielectric substrate is modelled as a cavity bounded by electric walls on the top and bottom. The basis for this assumption is the following observations for thin substrates ($h << \lambda$) [2].

• Since the substrate is thin, the fields in the interior region do not vary much in the *z* direction, i.e. normal to the patch.

• The electric field is *z* directed only, and the magnetic field has only the transverse components H_x and H_y in the region bounded by the patch metallization and the ground plane. This observation provides for the electric walls at the top and the bottom.

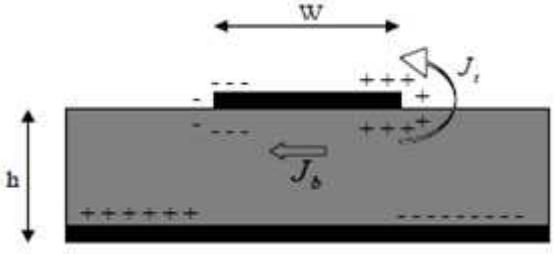

Figure 3.12 Charge distribution and current density creation on the microstrip patch

Consider Figure 3.12 shown above. When the microstrip patch is provided power, a charge distribution is seen on the upper and lower surfaces of the patch and at the bottom of the ground plane. This charge distribution is controlled by two mechanisms- an attractive mechanism and a repulsive mechanism as discussed by Richards [16]. The attractive mechanism is between the opposite charges on the bottom side of the patch and the ground plane, which helps in keeping the charge concentration intact at the bottom of the patch. The repulsive mechanism is between the like charges on the bottom surface of the patch, which causes pushing of some charges from the bottom, to the top of the patch. As a result of this charge movement, currents flow at the top and bottom surface of the patch. The cavity model assumes that the height to width ratio (i.e. height of substrate and width of the patch) is very small and as a result of this the attractive mechanism dominates and causes most of the charge concentration and the current to be below the patch surface. Much less current would flow on the top surface of the patch and as the height to width ratio further decreases, the current on the top surface of the patch would be almost equal to zero, which would not allow the creation of any tangential magnetic field components to the patch edges. Hence, the four sidewalls could be modelled as perfectly magnetic conducting surfaces. This implies that the magnetic fields and the electric field distribution beneath the patch would not be disturbed. However, in practice, a finite width to height ratio would be there and this would not make the tangential magnetic fields to be completely zero, but they being very small, the side walls could be approximated to be perfectly magnetic conducting [1].

Since the walls of the cavity, as well as the material within it are lossless, the cavity would not radiate and its input impedance would be purely reactive. Hence, in order to account for radiation and a loss mechanism, one must introduce a radiation resistance R and a loss resistance R_L. A lossy cavity would now represent an antenna and the loss is taken into account by the effective loss tangent δ_{eff} which is given as:

$$\delta_{eff} = 1/Q_T \tag{3.7}$$

Q_T is the total antenna quality factor and has been expressed by [8] in the form:

$$\frac{1}{Q_T} = \frac{1}{Q_d} + \frac{1}{Q_c} + \frac{1}{Q_r} \tag{3.8}$$

•Q_d represents the quality factor of the dielectric and is given as :

$$Q_d = \frac{\omega_r W_T}{P_d} = \frac{1}{\tan\delta} \tag{3.9}$$

where

ω_r is the angular resonant frequency.

W_T is the total energy stored in the patch at resonance.

P_d is the dielectric loss.

tanδ is the loss tangent of the dielectric.

• Q_e represents the quality factor of the conductor and is given as :

$$Q_c = \frac{\omega_r W_T}{P_c} = \frac{h}{\Delta} \tag{3.10}$$

where P_e is the conductor loss.

Δ is the skin depth of the conductor.

h is the height of the substrate.

• Q_r represents the quality factor for radiation and is given as:

$$Q_r = \frac{\omega_r W_T}{P_r} \tag{3.11}$$

where P_r is the power radiated from the patch.

Substituting equations (3.8), (3.9), (3.10) and (3.11) in equation (3.7), we get

$$\delta_{eff} = \tan\delta + \frac{\Delta}{h} + \frac{P_r}{\omega_r W_T} \tag{3.12}$$

Thus, equation (3.12) describes the total effective loss tangent for the microstrip patch antenna.

3.5.3 Full Wave Solutions-Method of Moments

One of the methods, that provide the full wave analysis for the microstrip patch antenna, is the Method of Moments. In this method, the surface currents are used to model the microstrip patch and the volume polarization currents are used to model the fields in the dielectric slab. It has been shown by Newman and Tulyathan [17] how an integral equation is obtained for these unknown currents and using the Method of Moments, these electric field integral equations are converted into matrix equations which can then be solved by various techniques of algebra to provide the result. A brief overview of the Moment Method described by Harrington [18] and [1] is given below.

The basic form of the equation to be solved by the Method of Moment is:

$$F(g) = h \tag{3.13}$$

where F is a known linear operator, g is an unknown function, and h is the source or excitation function. The aim here is to find g, when F and h are known. The unknown function g can be expanded as a linear combination of N terms to give:

$$g = \sum_{n=1}^{N} a_n g_n = a_1 g_1 + a_2 g_2 + \ldots\ldots + a_N g_N \tag{3.14}$$

where an is an unknown constant and gn is a known function usually called a basis or expansion function. Substituting equation (3.14) in (3.13) and using the linearity property of the operator F , we can write:

$$\sum_{n=1}^{N} a_n F(g_n) = h \tag{3.15}$$

The basis functions g_n must be selected in such a way, that each $F(g_n)$in the above equation can be calculated. The unknown constants a_n. cannot be determined directly because there are N unknowns, but only one equation. One method of finding these constants is the method of weighted residuals. In this method, a set of trial solutions is established with one or more variable parameters. The residuals are a measure of the difference between the trial solution and the true solution. The variable parameters are selected in a way which guarantees a best fit of the trial functions based on the minimization of the residuals. This is done by defining set of N weighting (or testing)

functions $\{w_m\} = w_1, w_2, ...w_N$ in the domain of the operator F. Taking the inner product of these functions.

$$\sum_{n=1}^{N} a_n \langle w_m, F(g_n) \rangle = \langle w_m, h \rangle \tag{3.16}$$

where $m = 1,2,.....N$

Writing in Matrix form as shown in [5], we get:

$$[F_{mn}][a_n] = [h_m] \tag{3.17}$$

Where

$$[F_{mm}] = \begin{bmatrix} \langle w_1, F(g_1) \rangle \langle w_1, F(g_2) \rangle ..... \\ \langle w_2, F(g_1) \rangle \langle w_2, F(g_2) \rangle ..... \\ \vdots \\ \vdots \end{bmatrix} \qquad [a_n] = \begin{bmatrix} a_1 \\ a_2 \\ a_3 \\ \vdots \\ a_N \end{bmatrix} \qquad [h_m] = \begin{bmatrix} \langle w_1, h \rangle \\ \langle w_2, h \rangle \\ \langle w_3, h \rangle \\ \vdots \\ \langle w_N, h \rangle \end{bmatrix}$$

The unknown constants a_n can now be found using algebraic techniques such as LU decomposition or Gaussian elimination. It must be remembered that the weighting functions must be selected appropriately so that elements of $\{ w_n \}$ are not only linearly independent but they also minimize the computations required to evaluate the inner product. One such choice of the weighting functions may be to let the weighting and the basis function be the same, that is,

$w_n = g_n$. This is called as the Galerkin's Method as described by Kantorovich and Akilov [19]. From the antenna theory point of view, we can write the Electric field integral equation as:

$$E = f_c(J) \tag{3.18}$$

where E is the known incident electric field.

J is the unknown induced current.

F_c is the linear operator.

The first step in the moment method solution process would be to expand J as a finite sum of

basis function given as:

$$J = \sum_{i=1}^{M} J_i b_i \tag{3.19}$$

where b_i is the i^{th} basis function and J_i is an unknown coefficient. The second step involves the defining of a set of M linearly independent weighting functions, w_j . Taking the inner product on

both sides and substituting equation (3.19) in equation (3.18) we get:

$$\langle w_j, E \rangle = \sum_{i=1}^{M} \langle w_j, f_e(J_i, b_i) \rangle \tag{3.20}$$

Where $j = 1,2,.....M$

Writing in Matrix form as,

$[Z_{ij}][J] = [Ej]$ (3.21)

Where

$Z_{ij} = < w_j , f e(b_i) >$

$Ej = < w_j , H >$

J is the current vector containing the unknown quantities.

The vector E contains the known incident field quantities and the terms of the Z matrix are functions of geometry. The unknown coefficients of the induced current are the terms of the J vector. Using any of the algebraic schemes mentioned earlier, these equations can be solved to give the current and then the other parameters such as the scattered electric and magnetic fields can be calculated directly from the induced currents. Thus, the Moment Method has been briefly explained for use in antenna problems.

Chapter 4

Triangular Patch Antenna

4.1 Introduction

The triangular microstrip antennas are one of the different shapes of microstrip antennas which have radiation properties similar to that of the rectangular antenna but with the advantage of being physically smaller [2].The simplest of triangular shapes is of equilateral. Equilateral triangular antenna is more directive antenna with compact size. It is important to determine the resonant frequencies of the antenna accurately because microstrip antennas have narrow bandwidths and can only operate effectively in the vicinity of the resonant frequency.

4.2. Triangular Patch Antenna Design-

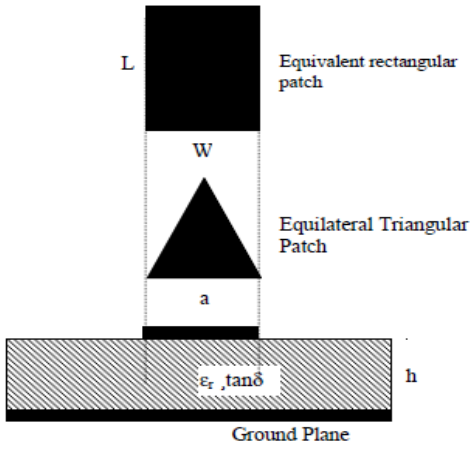

Fig.4.1. Equilateral Triangular Patch and Equivalent rectangular patch

Fig 4.1 shows an equilateral triangular patch and its equivalent rectangular patch antenna. The resonance frequency of the equilateral triangular patch can be determine by [10],

$$f_r = \frac{2\,c}{3\,L_{eff}\sqrt{\varepsilon^*_{r,dyn}}} \qquad (4.1)$$

Where, c is the velocity electromagnetic wave in free space. The L_{eff} is the effective length of the equivalent rectangular patch [L = a, W = (√3/2) a] and $\varepsilon^*_{r,dyn}$ is the dynamic relative permittivity of the triangular shown in Fig 4.1. The dynamic relative permittivity of the equivalent patch antenna is given by [20].

$$\varepsilon^*_{r,dyn} = \frac{C^*_{dyn}\left(\varepsilon^*_r, h, W\right)}{C^*_{dyn}\left(\varepsilon^*_r = 1, h, W\right)} \tag{4.2}$$

Where C^*_{dyn} is the complex dynamic capacitance of equivalent rectangular patch and

$$C^*_{dyn} = \frac{\varepsilon_0 \varepsilon^*_r A}{h \gamma_n \gamma_m} + \frac{1}{2\gamma_n}\left[\frac{\varepsilon^*_{reff}\left(\varepsilon^*_r, h, W\right)}{v_o Z\left(\varepsilon^*_r = 1, h, W\right)} - \frac{\varepsilon_0 \varepsilon^*_r A}{h}\right]$$

$$\gamma_j = \begin{cases} 1, & j = 0 \\ 2, & j \neq 0 \end{cases} \qquad j = n, m \tag{4.3}$$

Where, A is the area of equilateral triangular patch , the $Z(\varepsilon^*_r w , h)$ and $\varepsilon^*_{reff}(\varepsilon_r ,W, h)$ are the complex characteristics impedance and complex effective permittivity of the equivalent rectangular patch computed by using the closed form expression and ε^*_{reff} (ε_r , W , h) is equal to [21] ;

$$\varepsilon^*_{reff}(\varepsilon_r, W, h) = \frac{(\varepsilon_r + 1)}{2} + \left\{\frac{(\varepsilon_r + 1)}{2}\left(1 + \frac{12h}{a}\right)^{-\frac{1}{2}}\right\} \tag{4.4}$$

Where all the parameters have usual meaning

4.3 Resonant Frequencies of Triangular Patch

An expression to calculate the resonant frequencies of a triangular patch can be found in [10]. The expression considers the effect of a non-perfect magnetic wall, and was obtained by curve fitting the experimental and theoretical results for the resonant frequency for TM_{10} mode. The expressions are shown as follows:

$$f_{10} = \frac{2c}{3a_e\sqrt{\varepsilon_r}} \tag{4.5}$$

$$a_e = \left[1 + 2.199\frac{h}{a} - 12.853\frac{h}{a\sqrt{\varepsilon_r}} + 16.436\frac{h}{a\varepsilon_r} + 6.182\left(\frac{h}{a}\right)^2 - 9.802\frac{1}{\sqrt{\varepsilon_r}}\left(\frac{h}{a}\right)^2\right] \tag{4.6}$$

Accuracy of this empirical expression is claimed to be within 1% when compared with the value obtained from the moment method analysis [2]. Knowing the fundamental resonant frequency, f_{10}, the resonant frequency for higher order modes is given by:

$$f_{mn} = f_{10}\sqrt{m^2 + mn + n^2} \tag{4.7}$$

4.4 Methods of Analysis

There are many methods of analysis for microstrip antennas, the most popular methods are given as

- Transmission line model
- Cavity model
- Full wave model(Integral equation/moment methods)

Transmission line model is the easiest of all but it yields the least accurate results and it lacks the versatility because of fringing effects; electrically the patch of the microstrip antenna looks greater than its physical dimensions. Hence there is need to find the effective dielectric length. The patch is also comprised of radiating slots the equivalent admittance of each slot is derived as

$$Y_1 = G_1 + B_1 \tag{4.10}$$

Where G is the conductance.

From conductance we can find the input impedance

$$Z_{in} = \frac{1}{Y_{in}} = \frac{1}{\text{Total input admittance}}$$

Microstrip antenna resembles dielectric loaded cavities and they exhibit higher order resonances, the normalized field (between the patch and ground plane) can be found more accurately by treating that region as a cavity bounded by electric conductors (above and below) and by magnetic walls along the perimeter of the patch. When the electromagnetic energy propagates into the conducting patch through the coaxial cable some of the energy is reflected back into the coaxial cable and some of the energy gets radiated. The radiated energy can be calculated by getting the radiated field first. The radiated field is obtained by using field equivalence principle and image theory. Before

getting the radiating field first inside the cavity we need to find the field then the total cavity is assumed as a source and then the total electric field radiated is obtained. When the radiated field is obtained the radiated power is also obtained by poynting vector. This method is simple and versatile but requires large amount of computation. The limitation of this technique is usually speed and storage capacity of the computer.

The integral equation method with a moment method numerical solution will be introduced and used first to find the self and driving point impedance and mutual impedance of wire type of antenna. This method castes the solution for the induced current in the form of integral where the unknown induced current density is part of the integrand. Numerical techniques such as moment method [3] can then be used to solve the current density. In particular two classical integrations for linear elements, Pocklington's and Hallen's integral equations will be introduced, This approach is very general and it can be used with today's modern computational methods and equipment to compute the characteristics of complex configuration of antenna elements.

4.5 Field Representation

The field distribution in a triangular patch can be found using the cavity model, in which the triangle is surrounded by a magnetic wall along the Periphery. Consider a triangular resonator with magnetic side walls filled with a dielectric material of relative permittivity ϵ_r and thickness *s*ince $h << \lambda_0$, there is no variation of the fields along the *z*-direction. Therefore, the structure supports TM to Z modes. The solutions for the TE fields in an equilateral triangular waveguide with an electric boundary have been described by Schelkunoff [33] and Akaiwa [34]. The electric and magnetic field distributions for the TM_{mn} modes can be found as follows

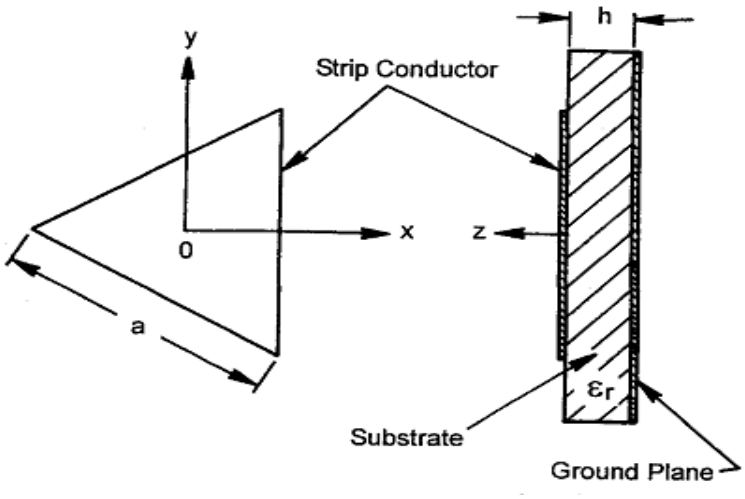

Fig 4.2 Configuration of an equilateral triangle microstrip antenna.

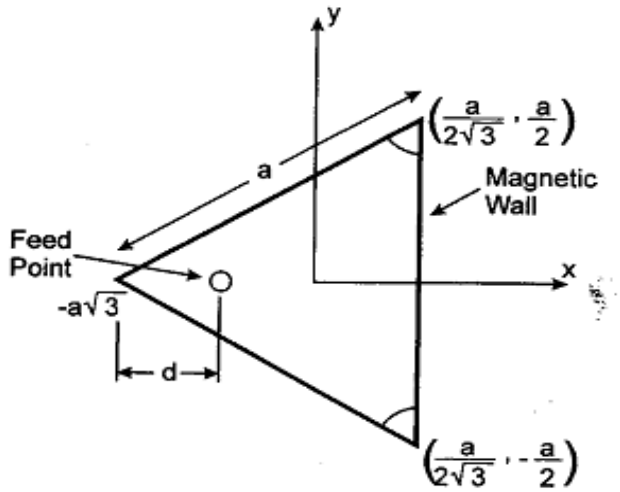

Fig 4.3 Triangular geometry with the coordinate system and the probe-feed.

Writing Maxwell's equations for the region under the patch we have,

$\nabla \times E = -j\omega\mu_0 H$ (4.8)

$\nabla \times H = -j\omega\varepsilon E + J$ (4.9)

$\nabla \cdot E = \frac{q}{\varepsilon}$ (4.10)

$\nabla \cdot H = 0$ (4.11)

Where

ε = permittivity of the substrate

µo = permittivity of free space

J = current density due to the feed

The fields in the interior region do not vary with X-axis or ($\frac{\delta}{\delta x} = 0$) ,The electric field is X directed only, hence the magnetic field has only the transverse component H_Y & H_Z in the region bounded by the patch metallization and the ground plane. This observation provides for the electric walls at the top and bottom. Because of dielectric is thin the field distribution in the interior region can be described by TM to X modes with $\frac{\delta}{\delta x} = 0$.

We know the Helmholtz wave equation as

$$\nabla\times\nabla\times E - K^2E = j\omega\mu_0 J \qquad (4.12)$$

$$\Rightarrow\nabla(\nabla\cdot E) - \nabla^2E - K^2E = -j\omega\mu_0 J \qquad (4.13)$$

$$\Rightarrow\nabla^2E + K^2E = j\omega\mu_0 J \qquad (4.14)$$

There exist only E_x component so putting E_x in the above equation

$$\Rightarrow\nabla^2E_x + K^2E_x = j\omega\mu_0 J$$

$$\Rightarrow\frac{\partial^2}{\partial x^2}(E_x) + \frac{\partial^2}{\partial y^2}(E_x) + \frac{\partial^2}{\partial z^2}(E_x) + K^2E_x = j\omega\mu_0 J$$

As $\frac{\partial^2}{\partial x^2}(E_x) = 0$

$$\Rightarrow\frac{\partial^2}{\partial y^2}(E_x) + \frac{\partial^2}{\partial z^2}(E_x) + K^2E_x = j\omega\mu_0 J$$

Now taking

$$E_x = A_{m,n,l}T(y,z)$$

For triangular patch antenna the Eigen function T(x, y) and after proper axis rotation the result obtained as

$$T(y,z) = \left(\cos\frac{2\pi y}{\sqrt{3}a} + \frac{2\pi}{3}\right)l \cdot \left(\cos\frac{2\pi Z(m-n)}{3a}\right) + \left(\cos\frac{2\pi y}{\sqrt{3}a} + \frac{2\pi}{3}\right)n \cdot \left(\cos\frac{2\pi Z(1-m)}{3a}\right) + \left(\cos\frac{2\pi y}{\sqrt{3}a} + \frac{2\pi}{3}\right)m \cdot \left(\cos\frac{2\pi Z(n-1)}{3a}\right) \qquad (4.15)$$

$A_{m,n,l}$ can be calculated by using Helmholtz wave equation and proper boundary condition.

One more concept is used that is ortho normalities of eigen function.
Mathematically as

$$\int_{-x}^{x}\int_{-y}^{y} T(y,z)dy.T^{*}(y,z)\,dy.dz = 1 \tag{4.16}$$

Where a is the equilateral triangle side length, Considering the dominant mode of triangular patch antenna as 1, 0,-1(As m=1, n=0, l=-1) the obtained T_{10} (y, z) is

$$T_{10}(y,z) = 2\left(\cos\frac{2\pi y}{\sqrt{3}a} + \frac{2\pi}{3}\right)\cdot\left(\cos\frac{2\pi Z}{3a}\right) + \left(\cos\frac{4\pi z}{3a}\right) \tag{4.17}$$

$$T_{10}^{2}(y,z) = \left\{2\left(\cos\frac{2\pi y}{\sqrt{3}a} + \frac{2\pi}{3}\right)\cdot\left(\cos\frac{2\pi Z}{3a}\right) + \left(\cos\frac{4\pi z}{3a}\right)\right\}^{2} \tag{4.18}$$

Now considering the field expression in the triangular Microstrip antenna We get

$$E_z = j\omega\mu\sum_{n=0}^{\infty}\sum_{m=0}^{\infty} C_{mn}\left\{\cos\frac{2\pi l y'}{\sqrt{3}a}.\ \text{Cos}\ \frac{2\pi(m-n)z}{3a} + \text{Cos}\frac{2\pi m y'}{\sqrt{3}a}\text{Cos}\frac{2\pi(n-l)z}{3a} + \text{Cos}\frac{2\pi n y'}{\sqrt{3}a}\cos\frac{2\pi(l-m)z}{3a}\right\} \tag{4.19}$$

Where the used mathematical notation significance is explained below

$y' = y + \frac{a}{\sqrt{3}}$

$C_{mn} = \frac{C'_{mn}}{k^2 - k_{mn}^2}$

$K_{mn} = \frac{4\pi}{3a}(m^2 + n^2 + mn)^{\frac{1}{2}}$

Where a is the side length of the triangular Patch.

$$C_{mn}^{**} = \begin{cases} \frac{4\sqrt{3}}{27a^2}(d+w)\ j_0\left(\frac{2\pi l}{\sqrt{3}a}(d+w)\right) + j_0\left(\frac{2\pi m}{\sqrt{3}a}(d+w)\right)] + j_0\left(\frac{2\pi n}{\sqrt{3}a}(d+w)\right) \\ -(d-w)\ j_0\left(\frac{2\pi l}{\sqrt{3}a}(d-w)\right) + j_0\left(\frac{2\pi m}{\sqrt{3}a}(d-w)\right)] + j_0\left(\frac{2\pi n}{\sqrt{3}a}(d-w)\right) \end{cases} \tag{4.20}$$

$$C_{mn}^{**} = \begin{cases} 1 & \text{if } m=n=0 \\ 6 & \text{if } (m=0\ \&\ n\neq 0) \text{ or } (m\neq 0\ \&\ n=0) \text{ or } (m=n\neq 0) \end{cases}$$

$$J_0(x) = \frac{\sin x}{x} \tag{4.21}$$

$$z_{in} = R + jx \tag{4.22}$$

$$Z_{in} = -j\omega\mu_0 \sum_{m=0}^{\infty}\sum_{n=0}^{\infty} \frac{4\sqrt{3}hC_{mn}^{**}}{27a_{eff}} \left\{ [\cos(\frac{2\pi ld}{\sqrt{3}a_{eff}}) j_0(\frac{2\pi lw}{\sqrt{3}a_{eff}}) + \cos(\frac{2\pi md}{\sqrt{3}a_{eff}}) j_0(\frac{2\pi mw}{\sqrt{3}a_{eff}}) \right.$$

$$\left. + \cos(\frac{2\pi nd}{\sqrt{3}a_{eff}}) j_0(\frac{2\pi nw}{\sqrt{3}a_{eff}})]^2 x \frac{(\omega^2 - \omega_{mn}^2)\mu_0\epsilon + j\delta_{\epsilon} k^2}{(\omega^2 - \omega_{mn}^2)(\mu_0\epsilon)^2 + (\delta_{\epsilon} k^2)^2} \right\} \quad (4.23)$$

Where

$$\delta_e = \frac{P_r + P_d + P_c}{2\omega W_E} \quad (4.24)$$

P_r = radiation loss

P_d = dielectric loss

P_c = copper loss

$2W_E$ = stored energy in the cavity

δ = loss tangent

Now,

$$K_{mn} = \frac{4\pi}{3a}(m^2 + n^2 + mn)^{\frac{1}{2}} \quad (4.25)$$

$$K_0 = \omega(\mu_0 \epsilon_0)^{\frac{1}{2}} \quad (4.26)$$

$$f_{mn} = \frac{2c}{3A\sqrt{\epsilon_r}}(m^2 + n^2 + mn)^{\frac{1}{2}} \quad (4.27)$$

The co-axial feed be located on the bisector line at a distance 'd' from the tip of the triangle. The X and Y co-ordinate are at (- $\frac{A}{\sqrt{3}}$, 0).The feed is modelled by a uniform current ribbon of some effective width 2w along the X axis.

Now simplifying the input impedance of triangular patch microstrip antenna to get the equivalent circuit. The general expression of input impedance is in the form of parallel combination of RLC circuit as

$$Z_{in} = \frac{1}{\frac{1}{R_1} + j\omega C_1 + \frac{1}{j\omega L_1}} \quad (4.28)$$

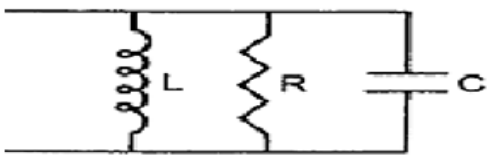

Fig 4.4 Equivalent circuit for triangular microstrip antenna

4.5 Design of Equilateral Triangular Patch Antenna.

The design starts with the selection of substrate; the substrate is selected according to requirement. Side length of patch a is determined next. this is governed by resonant frequency and the mode. Expression (4.5)-(4.7) are used for this purpose. For a more accurate design of a, one can use a full wave analysis such as the moment method.

Next, the feed location d is calculated such that the input resistance of the antenna matches the characteristics impedance of the feed line. For this purpose , the input resistance curve , similar to that of figure 4.5 , is developed from the input impedance expression, (4.23) , in this respect one need to calculate the total quality factor Q_T for the antenna , since $\delta_{eff} = 1/ Q_{T.}$ The value of total quality factor can be calculated.

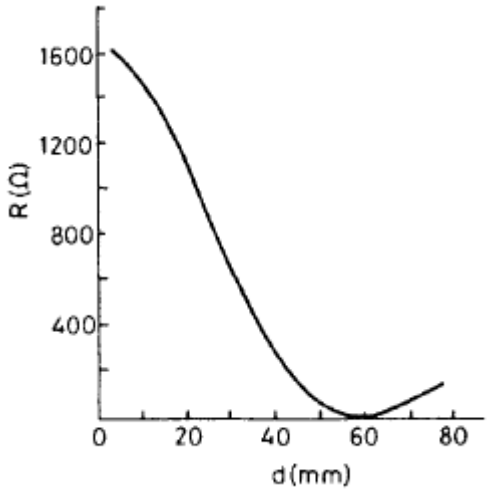

Figure 4.5 Input resistance as a function of feed position d of an equilateral patch with a=10cm, h=0.159cm , and $\varepsilon_r = 2.32$.

Chapter 5

Fractal Antenna

5.1 Introduction

Modern telecommunication system requires antennas with wider bandwidth and smaller dimensions than conventionally possible. Now days, the size of electronics systems has decreased drastically, whereas their functionality has increased. The antennas have not experienced the same evolution. The antenna size with respect to the wavelength is the parameter that will have influence on the radiation characteristics. For efficient radiation, the size should be of the order of a $\lambda/2$ or larger. But as antenna size reduces, the bandwidth, gain and efficiency of antenna deteriorate [22]. In addition the explosive growth in the wireless industry has renewed interest in multiband antennas. The most recent multiband antenna development is the incorporation of fractal geometry into radiators and the Sierpinski gasket antenna is a prime example. Since the Sierpinski gasket has proven itself to be an excellent multiband antenna, other multiband antennas can similarly be constructed using fractal geometry. The multi band and ultra wide band properties of antenna are due to their self-similarity of fractal geometry [24]-[25] while the space filling properties [26]-[27] of antenna leads to the miniaturization of antenna.

5.2 Fractal Antenna Geometry

Fractal antenna theory is built, as is the case with conventional antenna theory, on classic electromagnetic theory. Fractal antenna theory uses a modern (fractal) geometry that is a natural extension of Euclidian geometry. The effects of electromagnetic waves on fractal bodies have been intensively studied in recent years. Different from Euclidean geometries, fractal geometries have two common properties, space-filling and self-similarity. Self similar objects look roughly the same at any scale. Thus, in an antenna with fractal shape, similar surface current distributions are obtained for different frequencies, i.e. multiband behavior is provided. The space filling property, when applied to an antenna element, leads to an increase of the electrical length. The more convoluted and longer surface currents result in lowering the antenna resonant

frequency for a given overall extension of resonator. Therefore, given a desired resonance frequency, the physical size of the whole structure can be reduced.

In conventional microstrip patch antennas, dual or multi frequency operation can be achieved by using multiple radiating elements or reactively loaded patch antennas or multi-frequency dielectric resonator antennas. However in fractal antenna, self similarity property is used to achieve the same. The main advantages of fractal antenna over conventional antenna designs are its multiband operation & reduced size. Because of fractal loading present in this type of antenna, inductance & capacitance are added without the use of additional components. Antenna tuning units are also not required because these are 'self loading' antennas. Fractal antenna has useful applications in cellular telephone and microwave communications. HFSS is the industry standard for analyzing arbitrary 3D radiating elements such slot, horn, linear wire and patch antennas along with their polarization properties such as axial ratio, co- and cross-polarization. It automatically computes critical metrics such as gain, directivity, input impedance, efficiency, and near- and far-field radiation patterns.

HFSS can link field data between multiple HFSS models to capture the entire behavior of the Antenna system from transmitter to receiver. The applications of HFSS are Antenna systems, advanced package co-design for single and multi-chip integration, On-chip passives and High speed packages and interconnect.

5.3 Magnetic Field Patterns in Triangular Patch

The field distribution in a triangular patch antenna can be found using the cavity model. In this model, the triangular patch is surrounded by a magnetic wall along the sides. The expressions for the electric and magnetic field distributions for any TM_{mn} modes can be found in [22][23]. Using the expression for magnetic field distribution, the magnetic field patterns for various TM_{mn} modes, namely TM_{10}, TM_{11} , TM_{20}, TM_{21}, TM_{30} and TM_{31} are plotted in Figure 5.1.

.

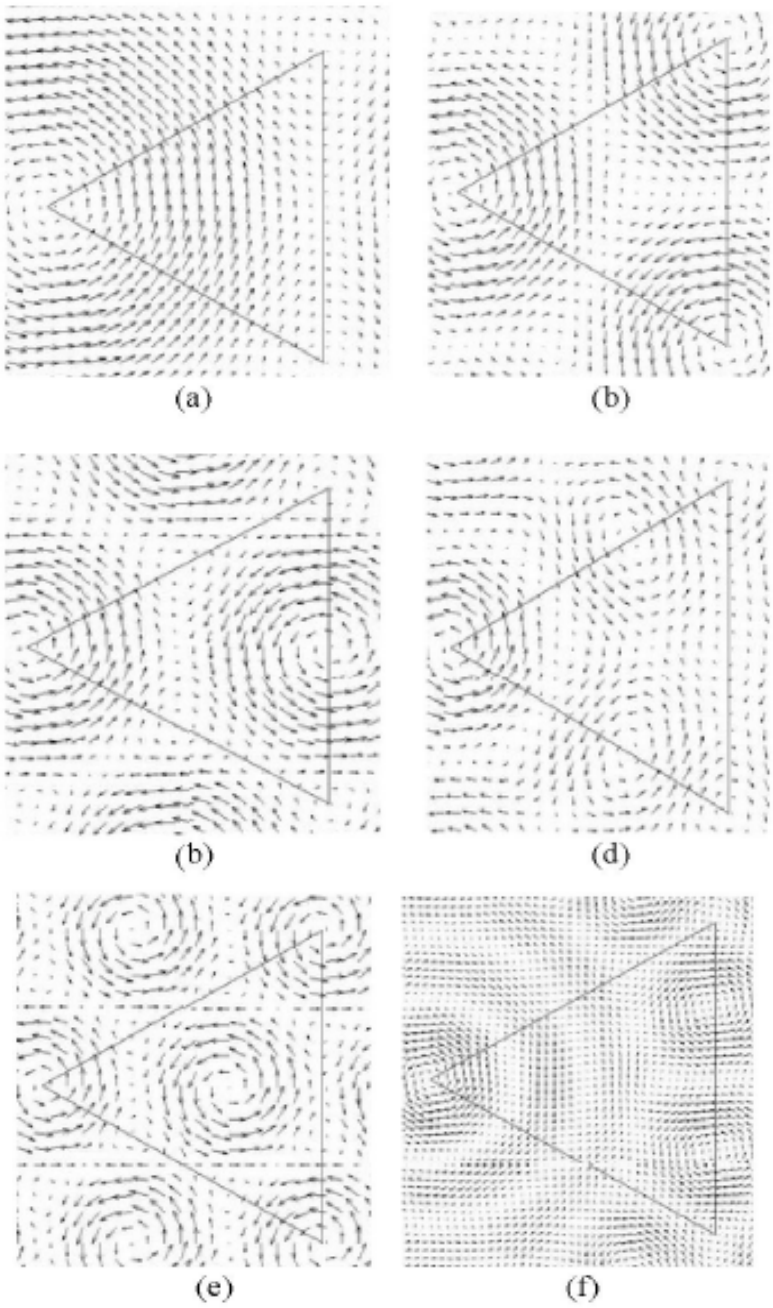

Figure 5.1 Magnetic field patterns of (a)TM_{1O}, (b)TM_{11}, (c)TM_{20}, (d)TM_{21}, (e)TM_{30}, (f)TM_{31}.

Thus, it is expected that by putting triangular slots nearby the null locations of the magnetic field pattern to introduce slight perturbation, the patch antenna will resonate better at the corresponding frequency with lower reflection loss. For example, if triangular slots are placed nearby the null locations of the TM21 magnetic field pattern, the slotted triangular patch antenna will resonate at TM21 mode with lower reflection loss than a conventional triangular patch.

5.4 Triangular Fractal Patch Configuration

So far, only the space saving benefits of fractal antennas have been exploited. There is another property of fractals that can be utilized in antenna construction. Fractals have self-similarity in their geometry, which is a feature where a section of the fractal appears the same regardless of how many times the section is zoomed in upon. Self-similarity in the geometry creates effective antennas of different scales. This can lead to multiband characteristics in antennas, which is displayed when an antenna operates with a similar performance at various frequencies. The generation of the fractal is shown in Fig. 5.2. A Sierpinski sieve dipole can be easily compared to a bowtie dipole antenna, which is the generator to create the fractal. The middle third triangle is removed from the bowtie antenna, leaving three equally sized triangles, which are half the height of the original bowtie. The process of removing the middle third is then repeated on each of the new triangles. For an ideal fractal, this process goes on for infinite no. of times.

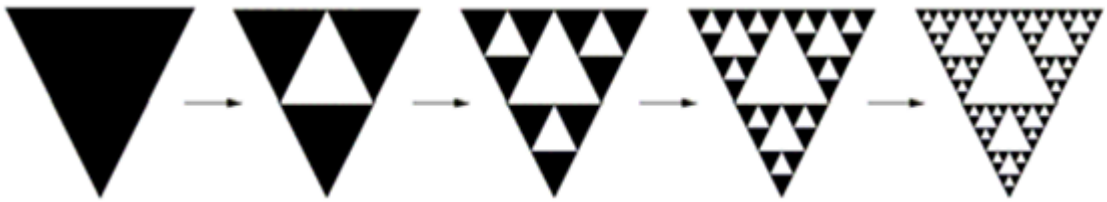

Fig.5.2 Generation of Sierpinski sieve

5.5 Advantages and Disadvantages

Advantages of fractal antenna technology are:

- Miniturazation
- Better input impedance matching
- Wideband/multiband (use one antenna instead of many)
- Frequency independent (consistent performance over huge frequency range)
- Reduced mutual coupling in fractal array antennas

Disadvantages of fractal antenna technology are:

- Gain loss
- Complexity
- Numerical limitations
- The benefits begin to diminish after few iterations.

5.6 Applications of Fractal Antennas

There are many applications that can benefit from fractal antennas. Discussed below are several ideas where fractal antennas can make a real impact. The sudden growth in the wireless communication area has sprung a need for compact integrated antennas. The space saving abilities of fractals to efficiently fill a limited amount of space create distinct advantage of using integrated fractal antennas over Euclidean geometry. Examples of these types of application include personal hand-held wireless devices such as cell phones and other wireless mobile devices such as laptops on wireless LANs and networkable PDAs. Fractal antennas can also enrich applications that include multiband transmissions. This area has many possibilities ranging from dual-mode phones to devices integrating communication and location services such as GPS, the global positioning satellites. Fractal antennas also decrease the area of a resonant antenna, which could lower the radar cross-section (RCS). This benefit can be exploited in military applications where RCS of the antenna is very crucial parameter.

Chapter 6

Result & Simulation

6.1 Rectangular Antenna-

A rectangular antenna which is resonating at 2.4 GHz is designed, in this antenna a rectangular patch of size 30 x 40 mm has been taken on the substrate of R.T Duroid of relative permittivity 2.2 and thickness 3.2 mm. All the structures have been simulated with the Ansoft HFSS 13 simulator. The procedure of simulation is as follows. The Rogers R.T Duroid 5880 (tm) dielectric with relative permittivity 2.2, thickness 3.2mm is taken. For feed, a coaxial probe-feed line is made to give a port for feed. Finally a radiation Box is placed over the antenna & thereafter the set up is simulated. The patch antenna contains a ground plane, substrate and radiating patch. The radiating part is connected with metal wire and ground plane is connected with outer part of coaxial cable. Here to design the 2.4 GHz Antenna specifications are as follows.

Length (L)	Width (W)	Height (h)	Permittivity (ε_r)
40 mm	30 mm	3.2 mm	2.2

Table 6.1 antenna design specification

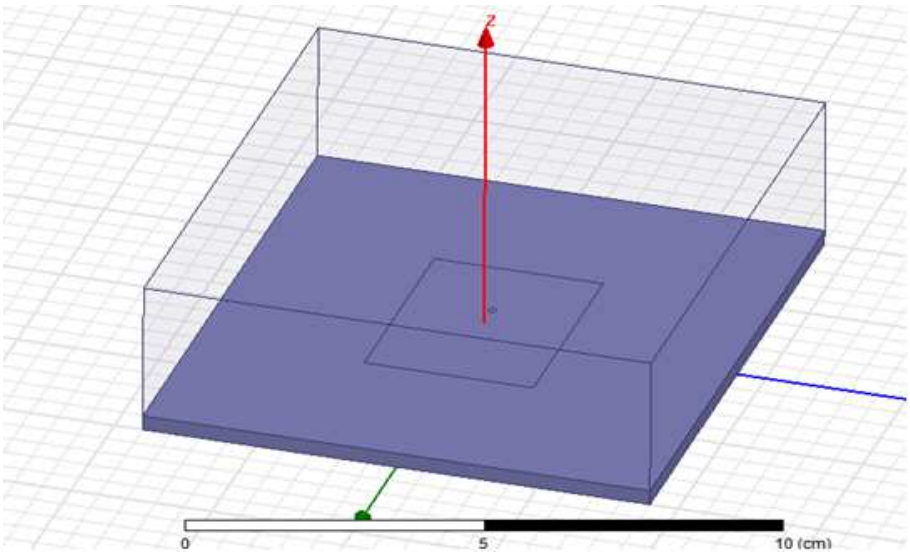

Fig 6.1- design of rectangular patch antenna

After simulating the antenna the results are obtained, some of the result like reflection coefficient (S_{11}) , VSWR, radiation pattern & gain polar plot are shown in figure 6.2.

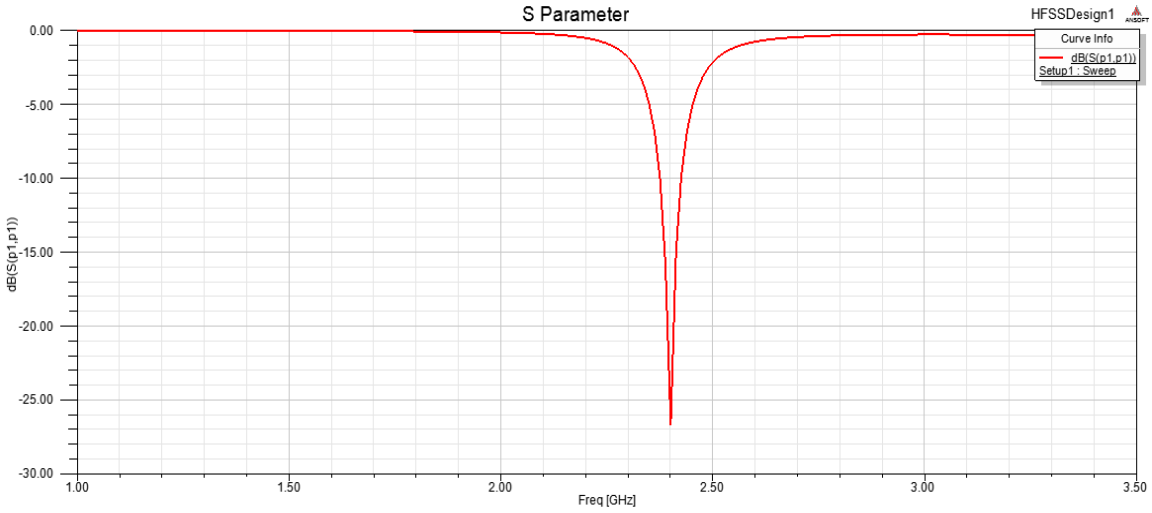

Fig 6.2- Reflection coefficient (S_{11}) of rectangular antenna

The S_{11} (Return loss) of the rectangular antenna has been plotted its return loss at 2.4 GHz is -27 dB. This is quiet good response it means that very less power is reflected & major portion of power is entering in the antenna. Now the radiation pattern of the antenna can also be plotted as shown below.

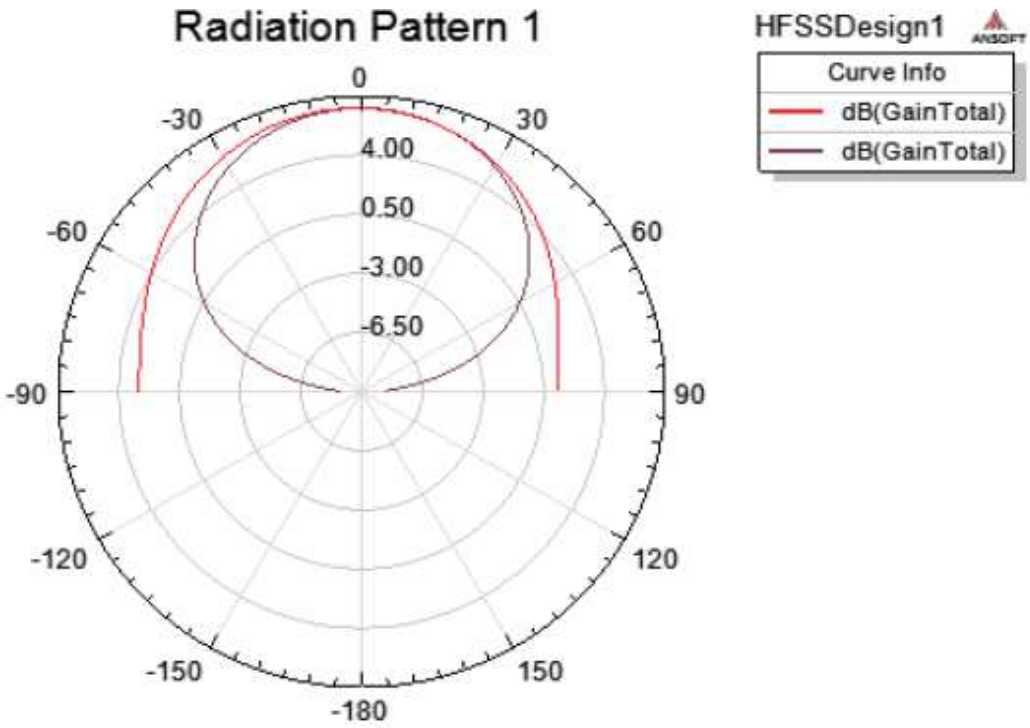

Fig 6.3- radiation pattern of rectangular antenna

The radiation pattern shows that the response of the antenna is mainly directed towards one direction, the response has been plotted for all theta(θ) values at phi(Φ) = 0^o & 90^o .

Now the 3-d polar plot of the antenna can also be plotted as shown below.

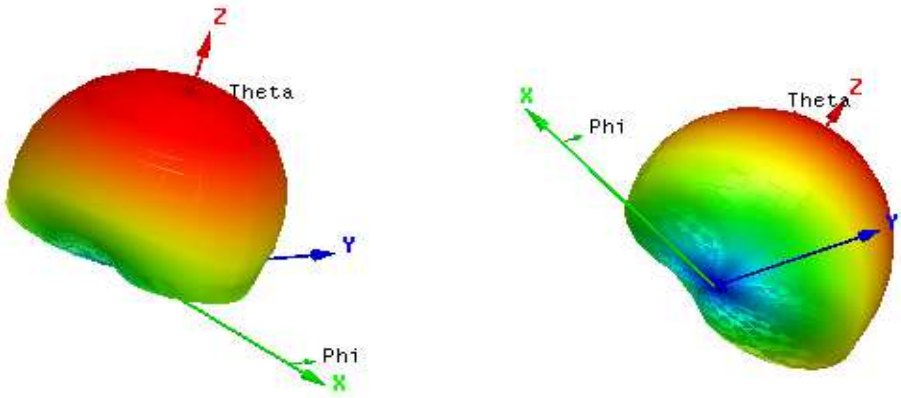

Figure 6.4- Gain polar plot of the antenna.

From the above polar plot also it is clear that the antenna is unidirectional, its various antenna parameter has been calculated by HFSS simulator at 2.4 GHz are shown below.

Directivity	Peak Gain	Efficiency
5.3336	5.2425	98.36%

Table 6.2 – Antenna output parameter

6.2 Triangular Patch Antenna

Triangular patch antenna of the same frequency as that of rectangular patch antenna, both theoretically & experimentally they are found to provide radiation characteristics similar to those of rectangular patches, but with a smaller size [2]. Here equilateral triangle patch antenna has been designed which is also resonating at 2.4 GHz. But this is having smaller size as compared to the rectangular patch antenna.

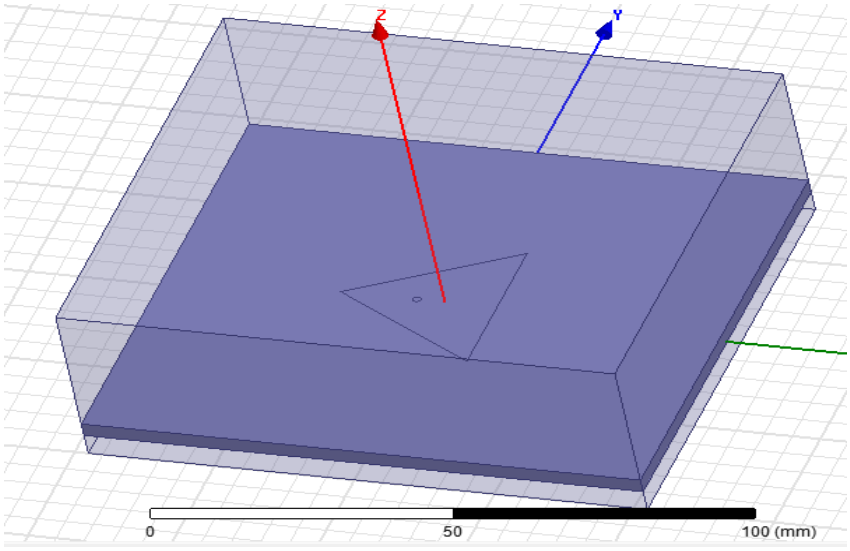

Fig 6.5 - triangular antenna design layout

The designed antenna is an equilateral triangular patch antenna of side length 32 mm. So we can see that the size of the antenna (i.e. area) has been decreased as compared to the rectangular patch antenna.

The S_{11} (Return loss) of this triangular antenna is plotted which also resonate at 2.4 GHz & having return loss -29 dB , but having small size. The directivity in this case is nearly same as compared to rectangular patch and efficiency is 96%.

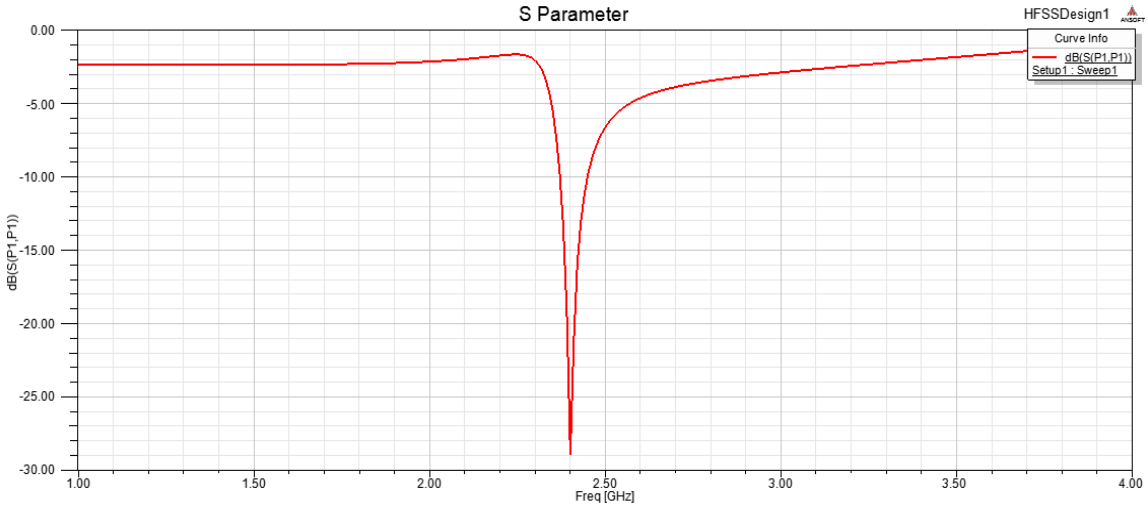

Fig 6.6 -the S_{11} (Reflection coefficient) of the triangular antenna.

Now the triangular slots have been made in the antenna, so it is a fractal antenna, which is shown below. The response of the fractal antenna is also shown in figure 6.8.

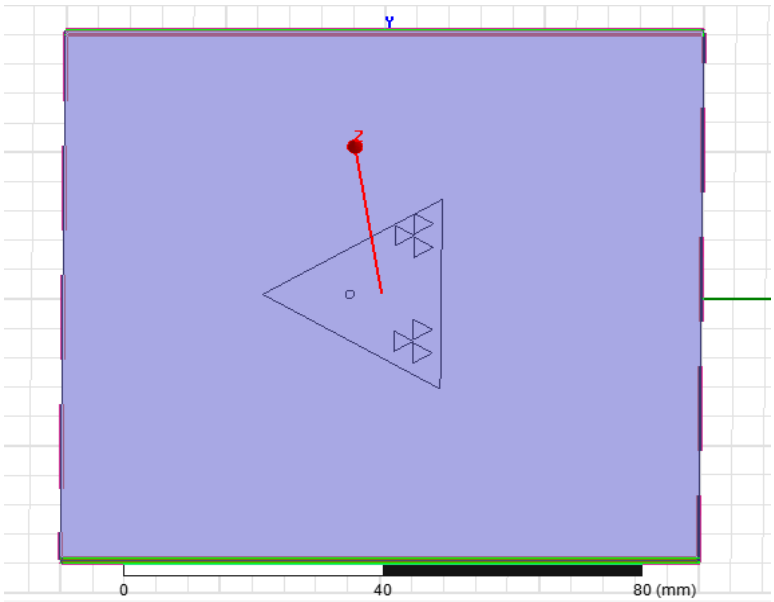

Figure 6.7- triangular antenna design-1 with 6 slots.

Now this antenna is simulated by using HFSS & the S_{11} Plot has been ploated , which shows that the reflection loss of the antenna at 2.4 GHz has been decreased upto -34db from -28db .

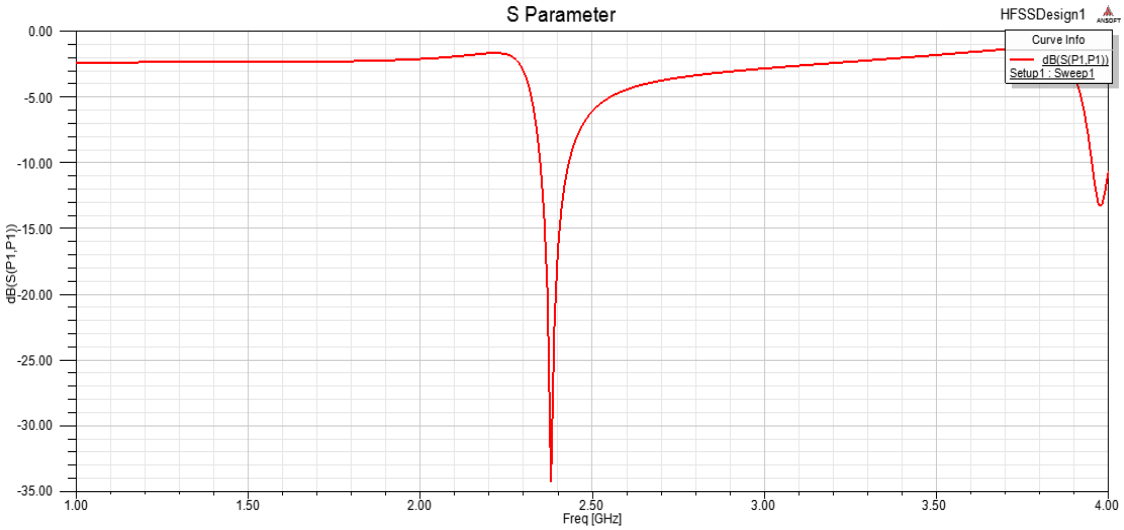

Figure 6.8 - the S_{11} (Reflection coefficient) of the triangular slotted antenna design 1.

Now again one more slot is made which is shown below & response is recorded.

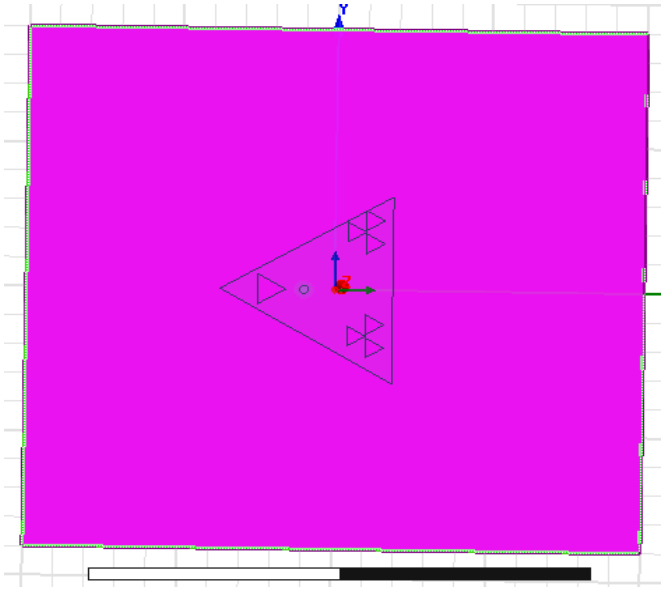

Figure 6.9- triangular antenna design 2 with 7 slots.

Here this fractal triangualr antenna is simulated & the S_{11} Parameter graph has been plotted , which showes that the reflection loss at 2.4GHz decreases upto -38db by using this fractal antenna.

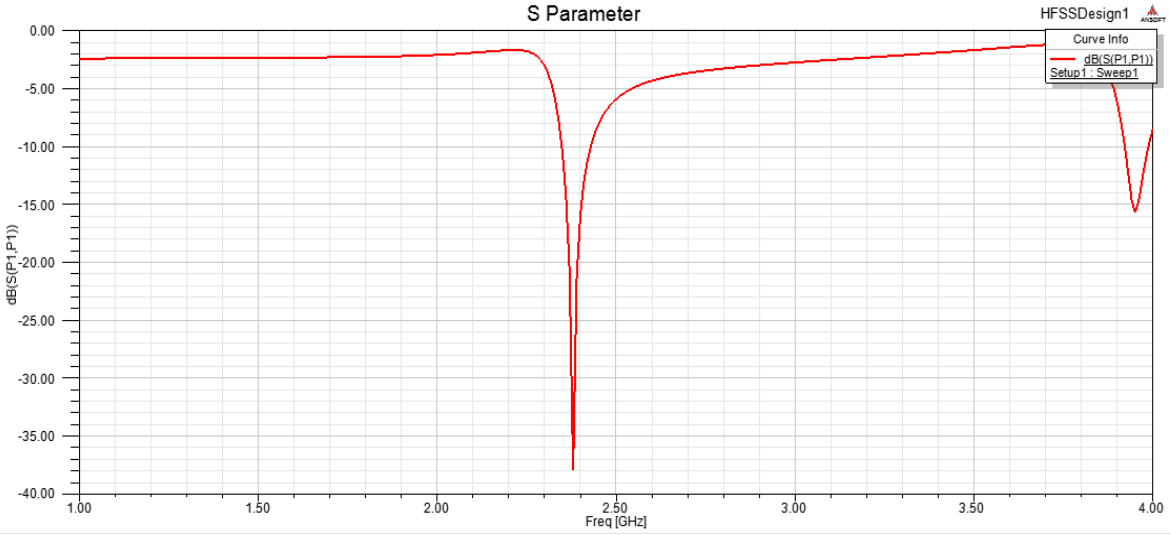

Figure 6.10- the S_{11} (Reflection coefficient) of the triangular slotted antenna design 2.

6.3 Multiband Triangular Patch Antenna

An equilateral triangular patch is reported to contain three broadside modes, TM_{10}, TM_{20}, and TM_{21} whereby radiation is in the broadside direction [31]. In [31], it was also pointed out that feeding the triangular patch, which has 100mm side lengths, at 47mm from the apex is suitable to excite all three broadside modes. This suggests that the equilateral triangular patch can be used as a multiband antenna operating at the resonant frequencies of these broadside modes with similar radiation pattern and polarization characteristics. It is shown that the reflection loss of the triangular patch at these broadside modes can be reduced by loading or placing triangular slots to perturb slightly the broadside modes' magnetic field pattern. This slight perturbation helps it to match better with the TM_{mn} magnetic fields. However, excessive perturbation to the magnetic field will obliterate the corresponding resonant frequencies. It is also shown that the reflection loss at other higher order resonant frequencies can also be reduced by placing these triangular slots at appropriate locations.

6.4 Simulation Studies

The patch antenna is simulated using HP High Frequency Structure Simulator (HFSS). its side length is 65 mm, and fed using a coaxial feed. The substrate thickness is 3mm with permittivity of 2.2 and an infinite ground plane is assumed, coaxial feed at 29 mm from the apex. The coaxial connector is modelled as a standard SMA connector with 50Ω characteristic impedance as shown in Figure 2, with r_o = 0.635mm, r_1 = 2.0574mm, e_1 = 2.07 and T = 20mm, [32]. The patch antenna is simulated from 0.1GHz to 5GHz with a delta error of 0.01 and 25MHz step size.

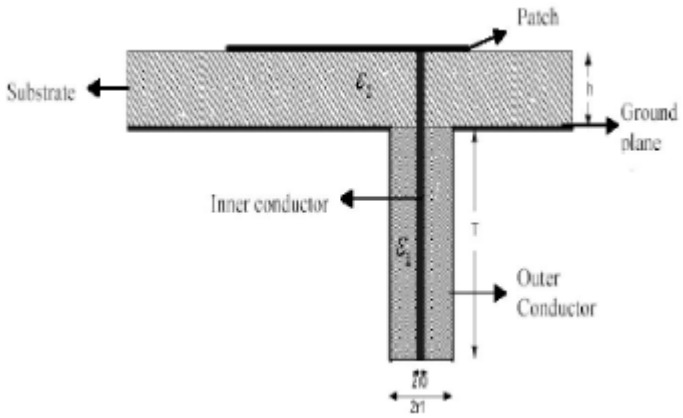

Figure 6.11: Cross section of the patch antenna.

6.5 Different Patch Configuration and Their Results

The first simulation is done by using a conventional triangular patch, fed at 29 mm from the apex. Then, triangular slots are placed to see the effects to its reflection loss. The results are recorded in reflection coefficient (S_{11}) magnitude against frequency curves.

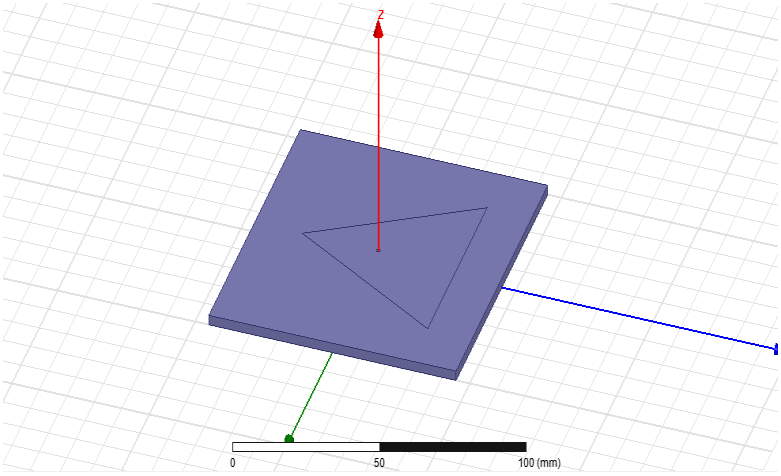

Figure 6.12 – traingular patch configuration

The S_{11}(return loss) of this antenna can be calculated by simulating the antenna in HFSS , so it is found that this antenna is having many bands with different reflection coefficients, which is shown below.

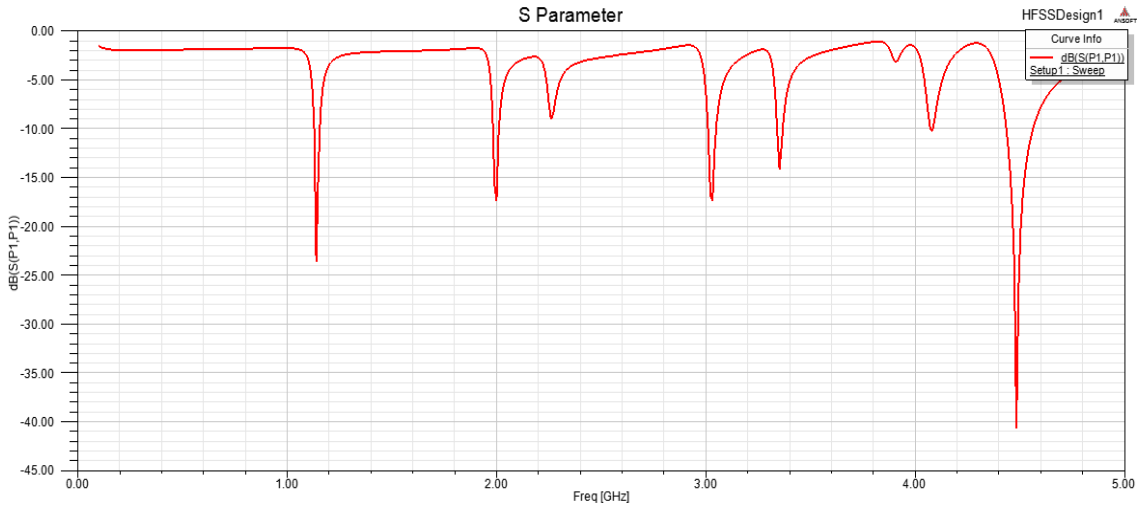

Fig 6.13- the magnitude of return loss(S_{11}) of traingular antenna

It is observed that the antenna is resonating at five frequencies, 1.1GHz, 2GHz, 3GHz, 3.2 GHz and 4.5 GHz, with reflection coefficient -24dB, -17dB, -17dB and -40 dB respectively.

It is also shown that the reflection loss at other higher order resonant frequencies can also be reduced by placing these triangular slots at appropriate locations. Now we will place the traingular slot at different location of traingular patch as shown below.

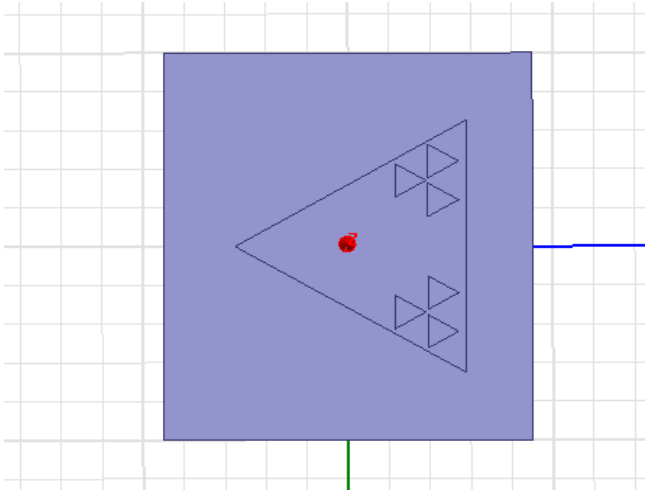

Figure 6.14 slotted patch configuration no.1

So the reflection loss will decrease at some of the frequency , like here the reflection loss at 1.1GHz , 2 GHz and 3GHz has been decreased as shown below.

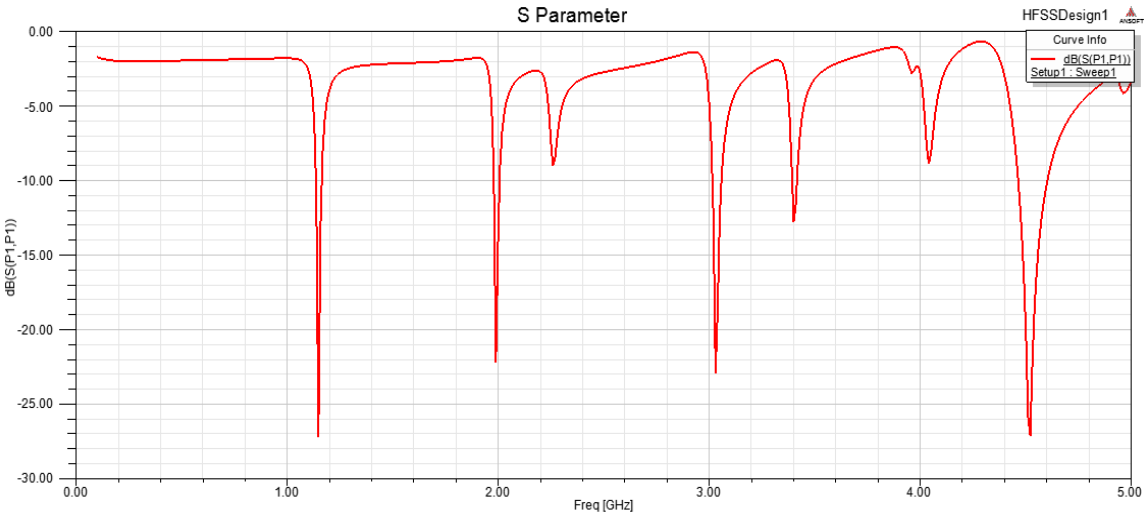

Fig 6.15- the magnitude of return loss(S_{11}) of slotted antenna 1.

In this case at the frequency 1.1GHz , 2GHz and 3GHz the return loss decreases & becomes -27dB, -22dB and -23dB respectively.

Now the slots has been placed in different way as shown below then again the response is observed now the response of the antenna will change.

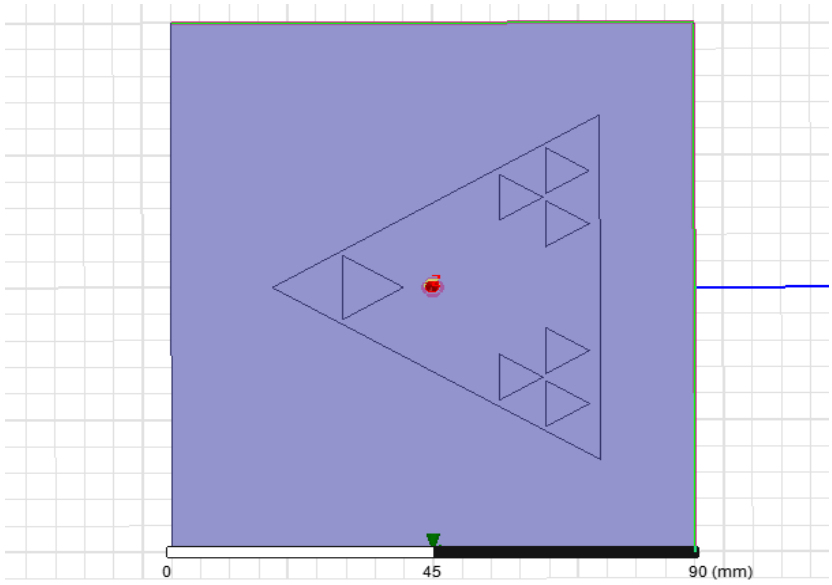

Figure 6.16 slotted patch configuration no.2

This slotted patch antenna structure is simulated on HFSS software and we will get the response (reflection coefficient) as shown below.

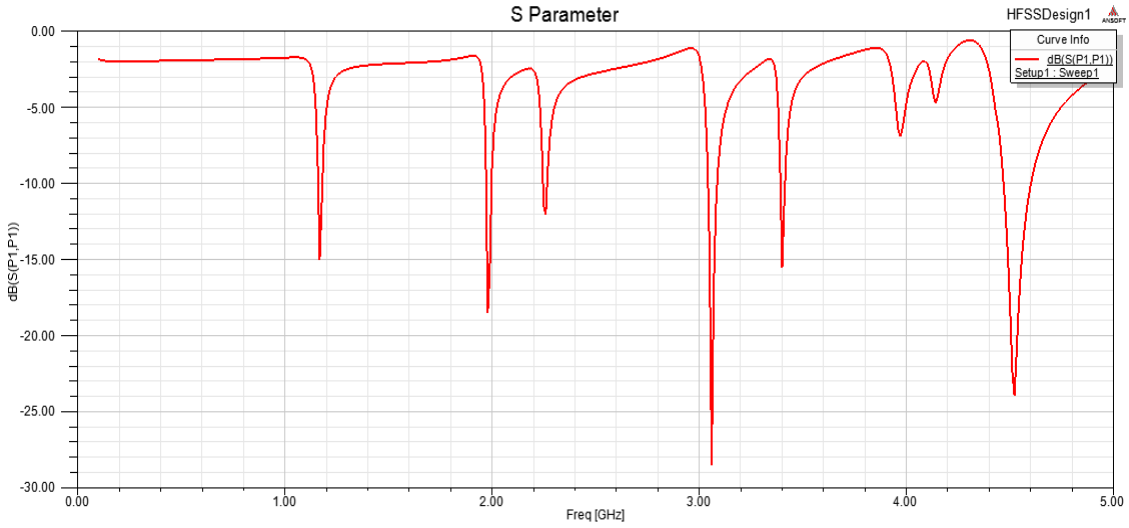

Fig 6.17- the magnitude of return loss(S_{11}) of slotted antenna 2.

Here the reflection loss at 3 GHz will decrease , its reflection coefficient decreases to -28.5 dB.

Again some slots are maid & observed that the reflection loss at many frequency will decrease.

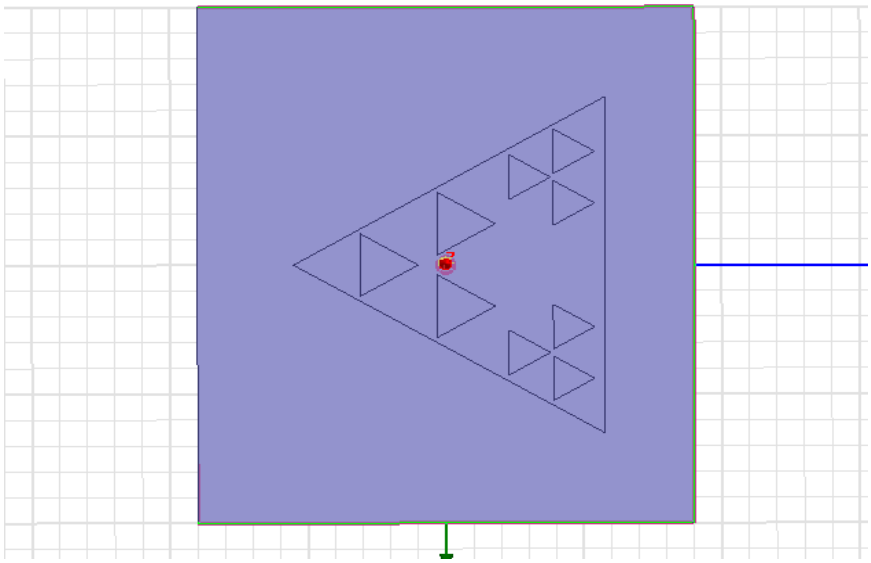

Figure 6.18 slotted patch configuration no.3

Now again this slotted patch antenna structure is simulated on HFSS software and we will get the response as shown below.

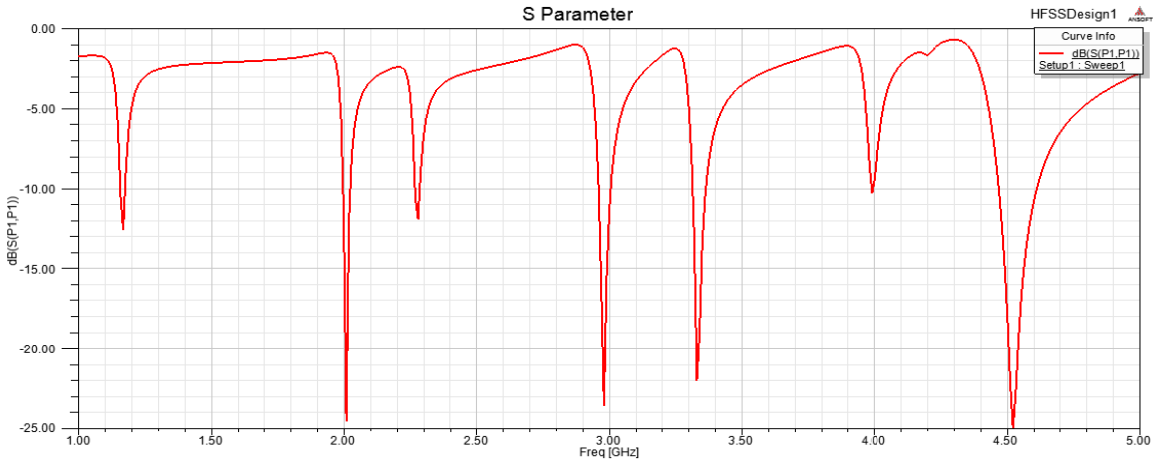

Fig 6.19- the magnitude of return loss(S_{11}) of slotted antenna 3.

In this slotted structure the reflection loss has been decreased at frequency 2GHz & 3 GHz which is -25dB and -24dB. also some new bands are introduced.

6.6 Result

From the above results we can see the advantage of the triangular antenna over the rectangular antenna has been analyzed that the size of the triangular antenna required for resonating at the same is less as compared to the rectangular patch antenna. For 2.4 GHz operating frequency the rectangular patch antenna of size 30×40 mm is required, whereas the size of the triangular patch antenna required is an equilateral triangular patch antenna of side length 32 mm, this is smaller than the rectangular patch antenna.

The other result is that by using the triangular slots in the triangular antenna i.e. by making it a fractal antenna we can achieve very less return loss as compared to the triangular antenna of the same size, this is shown below.

ANTENNA	RETURN LOSS
triangular antenna	-29dB
triangular antenna design with slots-1	-34dB
triangular antenna design with slots-2	-38dB

Table 6.3 Return loss comparison of different antenna

As we have studied in theoritical part that the reflection loss of the triangular patch at these broadside modes can be reduced by loading or placing triangular slots to perturb slightly the broadside modes' magnetic field pattern. This slight perturbation helps it to match better with the TM_{mn} magnetic fields. It is also shown that the reflection loss at other higher order resonant frequencies can also be reduced by placing these triangular slots at appropriate locations.

Here in case of the Multiband patch antenna designed we are getting 4 bands for wireless applications. Now to decrease the return loss we made the triangular slot which makes it a fractal antenna having less return loss at different frequencies. Various fractal design decreases the return loss at different frequencies.

We can draw a comparison table to show that the return loss of the antenna has been decreased at different frequency for different slotted antenna in Table 6.4.

	Reflection loss at different frequency(dB)		
Simulation cases	1.1 GHz	2GHz	3GHz
Triangular patch configuration	-24	-17	-17
slotted patch configuration 1	-27	-22	-23
slotted patch configuration 2	-15	-18	-28.5
slotted patch configuration 3	-13	-25	-24

Table 6.4- return loss of various antenna designs at different frequency.

So this has been also shown in the above results that the reflection loss decreases by placing the triangular slots on the triangular patch antenna or by making it as a fractal antenna.

Chapter 7

Conclusion

7.1 Conclusion

The objective of this work has been to

- Rectangular & Triangular Patch antenna resonating on 2.4 GHz is designed for Wi-Fi application & simulated on HFSS.
- It has been also shown experimentally that the size required for the triangular antenna to resonate at the same frequency is less as compared to the rectangular patch antenna with approximately same return loss, directivity and efficiency.
- In the equilateral triangular patch antenna the slots of the triangular shape has been made which forms the two design of fractal geometry.
- The first fractal geometry with 6 slots shows less return loss (-34dB) compared to the same dimension triangular patch antenna(with return loss -29dB) at 2.4 GHz
- The second fractal geometry with 7 slots shows less return loss (-38dB) compared to the same dimension triangular patch and first fractal geometry antenna at 2.4 GHz.
- The same concept of fractal is applied in the multiband triangular patch antenna. Also in this case after making the fractal geometry the return loss decreases at different frequency in various cases.
- In the multiband fractal antenna slotted patch configuration 1 the return loss is decreased at 1.1 GHz and 2 GHz with respect to the simple triangular patch antenna.
- It can be seen from the simulated results that in multiband fractal antenna slotted patch configuration 2 the return loss is decreased at 3 GHz.
- In case of the multiband fractal antenna slotted patch configuration 3 also the return loss is decreased at 2 GHz and 3 GHz , it can be seen from S_{11} plot.

7.2 Future Scope of present work

In future this project can be extended with following points:

- The antenna design has been implemented on software furthermore it can be fabricated and response can be analysed.
- This design can be used in any wireless application so their performance and response can be studied.
- Multiband antenna can be utilized for different frequency application according to their frequency bands it explore one antenna for different application.
- The fractal antenna of other shape can also be designed in the same way to get different frequency bands of other requirement.

REFERENCES

[1].Constantine A. Balanis, Antenna theory analysis and design, 2nd edition, John Wiley &sons, Inc, 1997.

[2] Garg, R., Bhartia, P., Bahl, I., Ittipiboon, A., Microstrip Antenna Design Handbook, Artech House, Norwood, MA, 2001

[3] Balanis, C.A., Advanced Engineering Electromagnetics, John Wiley & Sons, New York, 1989

[4] Stutzman, W.L. and Thiele, G.A., Antenna Theory and Design, John Wiley & Sons, Inc, 1998.

[5].WarrenL.Stutzman, Gary A.Thiele, Antenna Theory and Design,2nd edition, John Wiley & sons ,Inc,1998.

[6] Hammerstad, E.O., "Equations for Microstrip Circuit Design," Proc. Fifth European Microwave Conf., pp. 268-272, September 1975.

[7] Ulaby, F.T., Fundamentals of Applied Electromagnetics, Prentice Hall, 1999.

[8] Stutzman, W.L. and Thiele, G.A., Antenna Theory and Design, John Wiley & Sons, Inc, 1998.

[9] Kumar, G. and Ray, K.P., Broadband Microstrip Antennas, Artech House, Inc, 2003.

[10] R. Singh, A. De and R. S. Yadava, "comments on 'An improved formula for resonant frequency of the triangular microstrip patch antenna," IEEE Trans. Antennas Propagate, vol. AP-39, pp. 1443-1444, Sept. 1991.

[11] Qian, Y., et al., "A Microstrip Patch Antenna using novel photonic bandgap structures",

Microwave J., Vol 42, Jan 1999, pp. 66-76.

[12].Sophocles J. Orfanidis, Electromagnetic Waves and Antennas, ECE department,Rutgers University, 2004.

[13].Y.T.Lo and S.W.Lee, Antenna Handbook Theory, Application and Design, VanNostrandRenhold Company, New York, 1988.

[14] James, J.R. and Hall, P.S., Handbook of Microstrip Antennas, Vols 1 and 2, Peter Peregrinus, London, UK, 1989.

[15] Bahl, I.J. and Bhartia, P., Microstrip Antennas, Artech House, Dedham, MA, 1980

[16] Richards, W.F., Microstrip Antennas, Chapter 10 in Antenna Handbook: Theory

[17] Newman, E.H. and Tylyathan, P., “Analysis of Microstrip Antennas Using Moment Methods,” IEEE Trans. Antennas Propag., Vol. AP-29, No. 1, pp. 47-53, January 1981.

[18] Harrington. R.F., Field Computation by Moment Methods, Macmillan, New York, 1968.

[19] Kantorovich, L. and Akilov, G., Functional Analysis in Normed Spaces, Pergamon, Oxford,
pp. 586-587, 1964.

[20] A. K. Sharma and B. Bhatt, “Analysis of triangular microstrip resonator,” IEEE Trans. Microwave Theory Tech. vol. 30, pp. 2029-2031, Nov.1982.

[21] R. Garg and S. A. Long, “An improved formula for the resonant frequency of triangular microstrip patch antenna,” IEEE Trans. Antennas Propagat., vol. AP-36, p. 570, Apr.1988.

[22] Bahl, I. J., and P. Bhartia, Microstrip Antennas, ArtechHouse, Dedham, MA, 1980

[23] Helszajin, J., D. S. James and W. T. Nisbet, "Circulators Using Planar Triangular Resonators," IEEE Trans. On Microwave Theory and Techniques, Vol. MTT-27, 1979, pp. 188 193.

[24] C. Puente, J. Romeu, R. Pous, X. Garcia, and F. Benitez, “Fractal multiband antenna based on the Sierpinski gasket,” Electron. Lett., vol. 32, no. 1, pp. 1–2, Jan. 1996.

[25] C. Puente, J. Romeu, R. Pous, and A. Cardama, “On the behavior of the Sierpinski multiband fractal antenna,” IEEE Trans. Antennas Propagat., vol. 46, pp. 517–524, Apr. 1998.

[26] S. N. Khan, J. Hu, J. Xiong, and S. He, “Circular fractal monopole antenna for low VSWR UWB applications”, Progress in Electromagnetics Research Letters, Vol. 1, pp. 19–25, 2008.

[27] E. Lule, et al, “Koch island fractal ultra wideband dipole antenna”, IEEE, Antennas and Propagation Society International Symposium, Vol. 3, pp. 2516 – 2519, June 2004

[28] J. P. Gianviffwb and Y. Rahmat-Samii, “Fractal antennas: A novel antenna miniaturization technique and applications”, Antennas Propagate. Mag. Vol. 44, pp. 20–36, 2002.

[29] P. W. Tang and P. F. Wahid, “Hexagonal Fractal Multiband Antenna”, IEEE Antennas and Wireless Propagation Letters, Vol. 3, pp. 111-112, 2004.

[30] R. Kumar and P. Malathi, “Design of CPW –Fed Ultra wideband Fractal Antenna and Backscattering Reduction”, Journal of Microwaves, Optoelectronics and Electromagnetic Applications, Vol. 9, No. 1, pp. 10-19, June 2010

[31] K. F. Lee, K. M. Luk and J. S. Dahele, "Characteristics of the Equilateral Triangular Patch Antenna," IEEE Trans. On Antennas and Propagation, Vol. 36, 1988, pp. 1510-1518.

[32] Parikh, K., "Simulation of Rectangular Single Layer, Coax-Fed Patch Antennas Using Agilent High Frequency Structure Simulator (HFSS)", M.Sc. Thesis, Virginia Polytechnic Institute and State University, December 2003.

[33] S. A. Schelkunoff Electromagnetic Waves, pp.393 -397 1943 :Van Nostrand ,1943,p. 393.

[34] Y. Akaiwa "Operation modes of a waveguide Y circulator", IEEE Trans. Microwave Theory Tech., vol. MTT-22, pp.954 -960 1974